Self-Assembly of Novel [2]Catenanes and [2]Pseudorotaxanes Incorporating Thiacrown Ethers or Their Acyclic Analogues**

Masumi Asakawa, Peter R. Ashton, Wim Dehaen,* Gerrit L'abbé,† Stephan Menzer, Jan Nouwen, Françisco M. Raymo, J. Fraser Stoddart,* Malcolm S. Tolley, Suzanne Toppet, Andrew J. P. White, and David J. Williams*

Abstract: A series of π electron rich macrocyclic polythioethers and their acyclic analogues have been synthesized in good yields. The association constants for the complexation of the π electron deficient bis(hexafluorophosphate) bipyridinium-based salt, paraquat, by these macrocycles, as well as those for the complexation of corresponding acyclic compounds by the bipyridinium-based tetracationic cyclophane, cyclobis(paraquat-*p*-phenylene), are significantly lower than those observed in the case of the "all-oxygen" analogues. Nonetheless, yields as high as 86% were recorded in the template-directed syntheses of [2]catenanes composed of cyclobis(paraquat-*p*-phenylene) and the macrocyclic polythioethers. Single-crystal X-ray crystallographic analyses of the [2]catenanes incorporating constitutionally unsymmetrical π electron rich macrocyclic polythioethers revealed that, in all cases, the dioxyaromatic units are located inside the cavity of the tetracationic cyclophane component in preference to the dithiaaromatic units. A similar selectivity was observed in solution by variable-temperature ^{1}H NMR spectroscopy. However, inversion of the ratio between the two translational isomers of the two [2]catenanes bearing 1,5-dithianaphthalene, as one of their π electron rich ring systems, and either 1,4-dioxybenzene or 1,5-dioxynaphthalene, as the other, occurs upon increasing the temperature from −30 to +30 °C. These [2]catenanes can be viewed as temperature-responsive molecular switches.

Keywords
catenanes · molecular devices · pseudorotaxanes · self-assembly · translational isomerism

Introduction

In order to gain further insight into the fundamental principles governing the self-assembly of catenanes incorporating complementary dioxyarene-based π electron rich macrocyclic polyethers and bipyridinium-based π electron deficient tetracationic cyclophane components,[1] we have constitutional changes into the ring components of [2]catenanes of this type. In particular, the nature and substitution pattern of the dioxyarene ring systems incorporated within the π electron rich macrocycles, as well as the length and conformational mobility of the bridging polyether chains, have been modified.[2] Similarly, the nature of the recognition sites and of the bridging spacers located within the π electron deficient macrocyclic components have also been varied.[2] However, in the vast majority of cases, decreases in the yields associated with the template-directed syntheses[3] were observed relative to that achieved with the very first of this series of [2]catenanes, $\mathbf{1}\cdot 4PF_6$, which was self-assembled[4] in a yield of 70%.

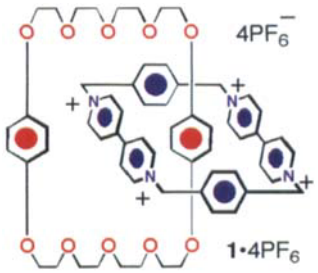

In order to improve further upon this yield, we have introduced thioether functions into the polyether chains of the π electron rich macrocyclic component of $\mathbf{1}\cdot 4PF_6$, since the π electron donor character of sulfur atoms differs from that of oxygen atoms. Also, thiacrown ethers are known to adopt conformations significantly different from those of their "all-oxygen" counterparts.[5] We report here 1) the syntheses and characterization of novel macrocycles in-

[*] Prof. J. F. Stoddart, Dr. M. Asakawa, P. R. Ashton, Dr. F. M. Raymo, M. S. Tolley
School of Chemistry, University of Birmingham
Edgbaston, Birmingham B152TT (UK)
Fax: Int. code +(121)414-3531
Dr. W. Dehaen, J. Nouwen, Dr. S. Toppet
Departement Scheikunde, Katholieke Universiteit Leuven
Celestijnenlaan 200F, 3001 Heverlee (Belgium)
Fax: Int. code +(16)32-79-90
Prof. D. J. Williams, Dr. S. Menzer, Dr. A. J. P. White
Department of Chemistry, Imperial College
South Kensington, London SW7 2AY (UK)
Fax: Int. code +(171)594-5804

[†] Professor L'abbé played a major role in the realization of the collaborative research reported in this paper, as well as in ensuring its production in manuscript form. Unfortunately, he did not live to see the results of this European collaboration reach print, an event he was so much looking forward to savouring when he died so suddenly and unexpectedly on 27 August, 1996.

[**] Molecular Meccano, Part 19; for Part 18, see: M. Asakawa, P. R. Ashton, C. L. Brown, M. C. T. Fyfe, S. Menzer, D. Pasini, C. Schever, N. Spencer, J. F. Stoddart, A. J. P. White, D. J. Williams, *Chem. Eur. J.* **1997**, *3*, in press.

0947-6539/97/0305-0772 $ 17.50+.50/0

corporating thioether functions along with their acyclic analogues, 2) their self-assembly into pseudorotaxane-like complexes in solution and in the solid state, and 3) the surprisingly efficient template-directed syntheses of a series of [2]catenanes incorporating cyclobis(paraquat-*p*-phenylene) and these macrocyclic polythioethers.

Results and Discussion

Synthesis: Tetrathiacrown **2** was prepared in low yield (5%) by treating 1,4-bis(2-bromoethoxy)benzene with bis(2-mercaptoethyl)ether in the presence of K_2CO_3 as the base (Scheme 1). By employing Cs_2CO_3 instead, only a small increase in the yield (from 5 to 7%) of the macrocyclization was observed. In both instances, the ansa compound **3** was obtained as the major product in yields of 31 and 46% when K_2CO_3 and Cs_2CO_3, respectively, were employed.

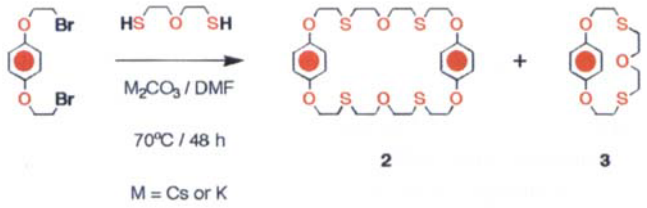

Scheme 1. Synthesis of the π electron rich macrocycle **2**.

The isomeric tetrathiacrown **4** was synthesized as illustrated in Scheme 2. Reaction of 4-aminothiophenol with tetraethyleneglycol dichloride was followed

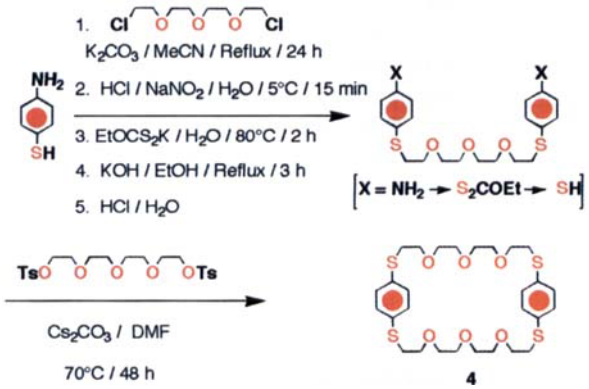

Scheme 2. Synthesis of the π electron rich macrocycle **4**.

by diazotization. The resulting bisdiazonium salt was treated with $EtOCS_2K$, and the subsequent hydrolysis gave the corresponding dithiol. Macrocyclization of this dithiol with tetraethyleneglycol bistosylate in the presence of Cs_2CO_3 afforded the macrocycle **4** in a yield of 24%.

Tetrathiacrown **5** was synthesized in low yield (7%) by means of a [2+2] macrocyclization (Scheme 3), starting from 1,5-naphthalenedithiol and tetraethyleneglycol ditosylate in the presence of either K_2CO_3 or Cs_2CO_3 in DMF. Once again, the ansa compound **6** was obtained as the major product (47%).

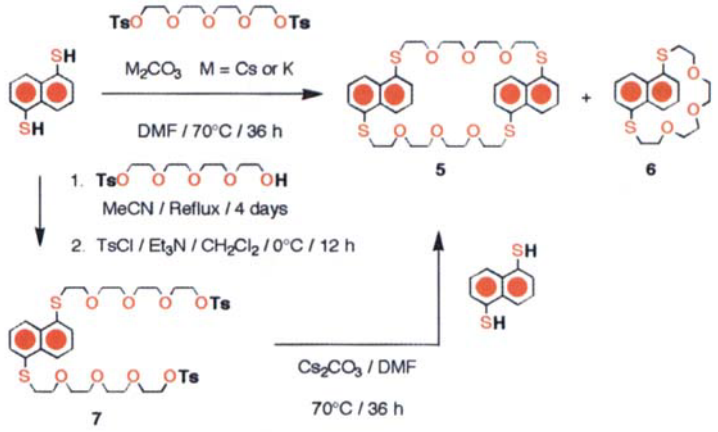

Scheme 3. Synthesis of the π electron rich macrocycle **5**.

Alternatively, **5** was prepared in a three-step synthetic route involving 1) alkylation of 1,5-naphthalenedithiol with tetraethyleneglycol monotosylate, 2) conversion of the resulting diol into the bistosylate **7**, and 3) [1+1] macrocyclization performed in the presence of Cs_2CO_3, which gave **5** in a yield of 39%.

Similarly, the bistosylates **8** and **9** were treated with 1,5-naphthalenedithiol to give the unsymmetrical macrocycles **10** (35%) and **11** (22%), respectively (Scheme 4). Macrocyclization of **8**

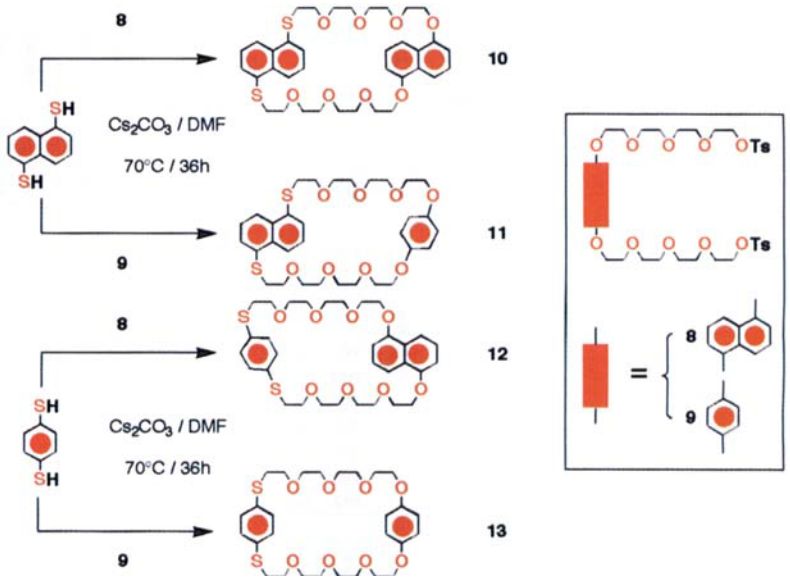

Scheme 4. Synthesis of the π electron rich macrocycles **10**–**13**.

and **9** with 1,4-benzenedithiol afforded instead the unsymmetrical macrocycles **12** (22%) and **13** (23%), respectively.

The acyclic compounds **14** and **15** were prepared by alkylation of the corresponding thiol and phenol, respectively, with 2-(2-methoxyethoxy)ethyl chloride under standard conditions (Scheme 5). The isomeric thioethers **16** and **17** were obtained from appropriate 1,5-dihydroxynaphthalene derivatives, as shown in Scheme 5.

The [2]catenanes **19**·4PF_6–**23**·4PF_6 were self-assembled according to two different synthetic procedures. In one case, the

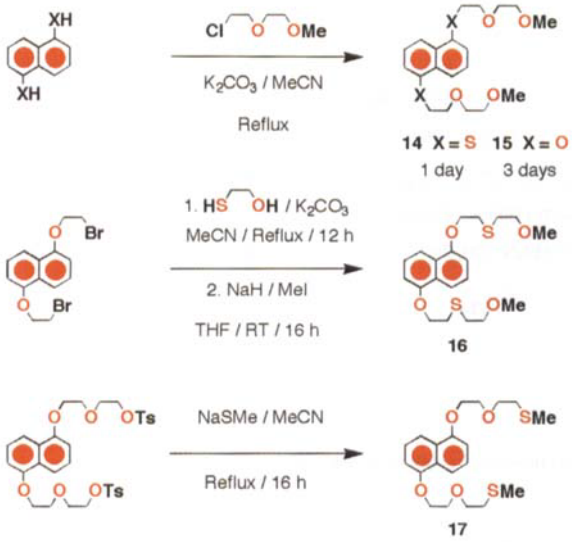

Scheme 5. Synthesis of the 1,5-disubstituted naphthalene-based compounds **14**–**17**.

bis(hexafluorophosphate) salt **18**·2PF$_6$ was treated with 1,4-bis(bromomethyl)benzene in the presence of 2.5 molar equivalents of one of the π electron rich macrocycles, either **5**, **10**, or **11**, to afford the corresponding [2]catenanes in yields of 47, 60, and 50%, respectively (Scheme 6). Alternatively, the reaction was

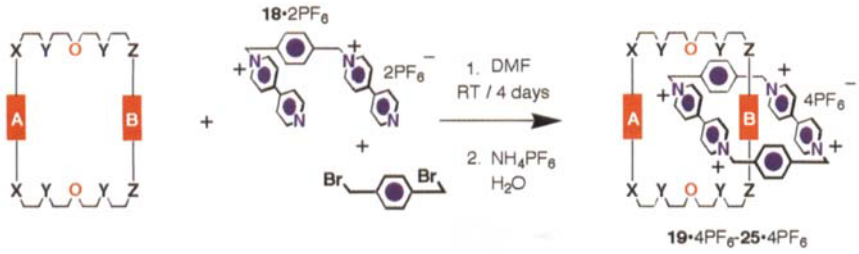

Macrocycle	X	Y	Z	A	B	[2]Catenane
2	O	S	O	HQ	HQ	19·4PF$_6$
4	S	O	S	HQ	HQ	20·4PF$_6$
5	S	O	S	NP	NP	21·4PF$_6$
10	S	O	O	NP	NP	22·4PF$_6$
11	S	O	O	NP	HQ	23·4PF$_6$
12	S	O	O	HQ	NP	24·4PF$_6$
13	S	O	O	HQ	HQ	25·4PF$_6$

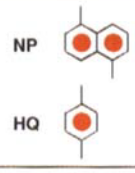

Scheme 6. Self-assembly of the [2]catenanes **19**·4PF$_6$–**25**·4PF$_6$.

performed employing a sixfold excess of **18**·2PF$_6$ and 1,4-bis(bromomethyl)benzene with respect to one of the π electron rich macrocycles, either **5**, **10**, or **11**, to afford the corresponding [2]catenanes in yields of 70, 77, and 65%, respectively. As a result of the improved yields, the second procedure was used also in the case of the macrocycles **12** and **13**, which gave the corresponding [2]catenanes **24**·4PF$_6$ and **25**·4PF$_6$ in yields of 86 and 53%, respectively. The yields achieved in the case of the [2]catenanes **22**·4PF$_6$ and **24**·4PF$_6$—namely, 77 and 86%—are among the highest ever obtained for such self-assembly processes,[6] and open up the possibility of making [2]catenanes in gram-scale quantities. Surprisingly, in the case of the macrocycles **2** and **4**, no catenated products were obtained by performing the reactions under otherwise identical conditions. However, by employing ultrahigh pressure conditions (12 kbar), the [2]catenane **20**·4PF$_6$ was obtained in a yield of 15%, starting from **4**, while only traces of **19**·4PF$_6$ were detected when the macrocycle **2** was used.

X-Ray Crystallography: The X-ray analysis revealed that, in the solid state, **2** adopts an open but flattened conformation (Figure 1), with the centers of the two hydroquinone rings separated

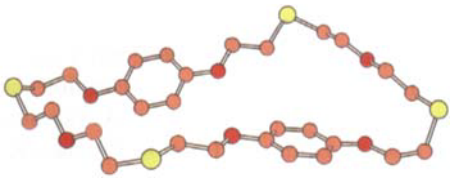

Figure 1. Geometry adopted by the π electron rich macrocycle **2** in the solid state.

by 6.99 Å. The most striking conformational features are 1) the coplanar all-*anti* geometries associated with both the $SCH_2CH_2OCH_2CH_2S$ linkages and 2) the coplanarity of the hydroquinone rings with, in one direction, their attached OCH_2CH_2 groups and in the other, their attached OCH_2CH_2S groups. Within these latter two portions of the macrocycle, the $CH_2OC_6H_4OCH_2$ units have a *syn* geometry. Inspection of the packing of the molecules shows a marked absence of any intermolecular hydrogen bonds or aromatic–aromatic interactions.

The X-ray structural investigation shows **10** to crystallize with two crystallographically independent molecules in the unit cell. Each molecule is positioned about a crystallographically independent symmetry center. Thus, it is not possible to distinguish between the sites occupied by the oxygen and sulfur atoms attached to the 1,5-disubstituted naphthalene units. Fifty percent of the time they are positioned on one naphthalene ring system within the macrocycle and 50% on the other, as averaged throughout the whole crystal. Both macrocycles have similar conformations, namely, self-filling with parallel overlap of their 1,5-disubstituted naphthalene ring systems, as shown in Figure 2. The conformation observed for **10** is in marked contrast to the one we have reported previously in the literature[7] for the "all-oxygen" analogue in which the two 1,5-dioxynaphthalene units are inclined orthogonally with respect to each other. Again, we see no evidence for any intermolecular π–π stacking interaction, [C–H···O] hydrogen bonding, or [C–H···π] interactions.

In the crystalline state, **20**·4PF$_6$ has a structure (Figure 3) possessing C_2 crystallographic symmetry about an axis passing through the centers of the two 1,4-dithiabenzene rings. The only major difference between **20**·4PF$_6$ and its "all-oxygen" analogue[8] **1**·4PF$_6$ is the adoption of an *anti* geometry for the

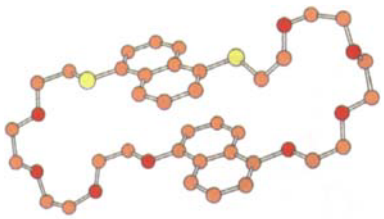

Figure 2. Geometry adopted by the π electron rich macrocycle **10** in the solid state.

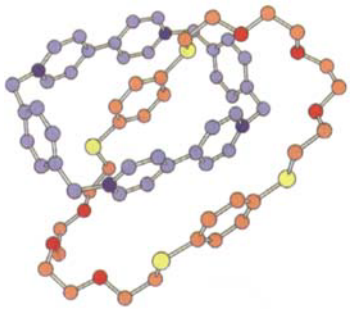

Figure 3. Geometry adopted by the [2]catenane **20**·4PF_6 in the solid state.

"outside" $CH_2SC_6H_4SCH_2$ unit (in the "all-oxygen" case, the *syn* geometry is adopted). The "inside" $-SC_6H_4S-$ vector is inclined by 48° to the mean plane of the tetracationic cyclophane, while the "outside" one is inclined by 21°. The mean interplanar separations between the "inside" phenylene ring and the "outside" and "inside" bipyridinium units are 3.48 and 3.54 Å, respectively; the equivalent separation between the "outside" phenylene ring and the "inside" bipyridinium unit is 3.42 Å. The other significant stabilizing interactions are [C–H···π] contacts ([H···π] 2.83 Å; [C–H···π] 163°) between the "inside" phenylene ring and the *p*-xylene spacers of the cyclophane. The molecules of the [2]catenane pack to form polar stacks along the crystallographic twofold axis (Figure 4). In these stacks, the mean interplanar separation between the "outside" phenylene ring of one molecule and the "outside" bipyridinium unit of an adjacent [2]catenane is 3.40 Å.

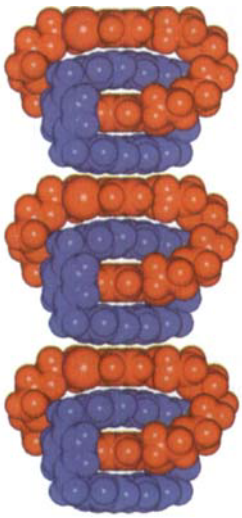

Figure 4. Packing diagram of the [2]catenane **20**·4PF_6 showing the donor–acceptor polar stack formed in the crystal.

Like its "all-oxygen" counterpart, the [2]catenane **21**·4PF_6, incorporating a polyether macrocycle containing two 1,5-dithianaphthalene residues, crystallizes in a triclinic unit cell with very similar overall dimensions (Figure 5). The mean interplanar separations between the "inside" naphthalene ring and the "outside" and "inside" bipyridinium units are 3.38 and 3.42 Å, respectively; the equivalent separation between the "outside" naphthalene ring and the "inside" bipyridinium unit is 3.40 Å. The angle between the $-SC_{10}H_6S-$ axes of the "inside" and "outside" naphthalene residues and the mean plane of the tetracationic cyclophane are 48 and 30°, respectively.

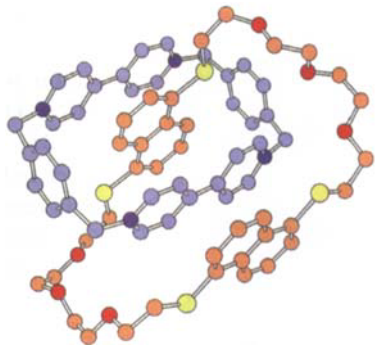

Figure 5. Geometry adopted by the [2]catenane **21**·4PF_6 in the solid state.

It is interesting to note that, in both this structure and that of its "all-oxygen" analogue, the "inside" and "outside" naphthalene rings are "flipped" with respect to each other about a "C_2 axis" that runs normal to the molecular "C_2 axis", which passes through the centers of the two naphthalene rings and the two bipyridinium units. In this [2]catenane, the π–π stacking interactions are assisted by a combination of [C–H···π] interactions and [C–H···O] hydrogen bonds. The former involve the hydrogen atoms on the C-4 and C-8 positions of the "inside" naphthalene rings and their proximal *p*-xylene spacers in the cyclophane ([H···π] 2.57, 2.58 Å; [C–H···π] 146, 145°). The latter are between one of the *p*-phenylene hydrogen atoms in each *p*-xylene unit and their adjacent central oxygen atoms of the polythioether linkages ([C···O] 3.30, 3.36 Å; [H···O] 2.36, 2.47 Å; [C–H···π] 168, 160°). In the crystal, the [2]catenane molecules pack to form conventional lattice-translated stacks with an interplanar separation between "outside" naphthalene rings of one molecule and the "outside" bipyridinium unit of the other of 3.33 Å.

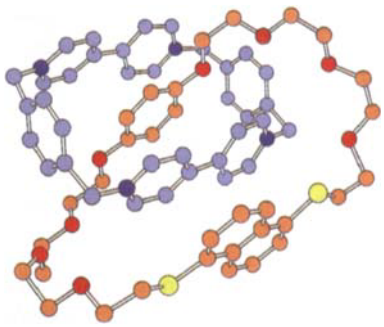

Figure 6. Geometry adopted by the [2]catenane **23**·4PF_6 in the solid state.

In the crystal structure of **23**·4PF_6 (Figure 6), where the macrocyclic polythioether contains a hydroquinone ring and a 1,5-dithianaphthalene residue, the hydroquinone ring is positioned in the "inside" of the tetracationic cyclophane and the 1,5-disubstituted naphthalene ring on the "outside". The tilt angle of the $-OC_6H_4O-$ axis of the "inside" hydroquinone ring to the mean plane of the tetracationic cyclophane is 48°, whereas that of the $-SC_{10}H_6S-$ vector of the "outside" 1,5-disubstituted naphthalene ring system is 30°. The mean interplanar separations between the "inside" hydroquinone ring and the "outside" and the "inside" bipyridinium units are 3.45 and 3.41 Å, respectively. The separation between the "outside" naphthalene ring system and the "inside" bipyridinium unit is 3.45 Å. Secondary stabilization of the π–π–π–π [2]catenane structure is achieved by a combination of 1) [C–H···π] interactions between the "inside" hydroquinone ring and the two *p*-xylene spacers of the cyclophane ([H···π] 2.76, 2.96 Å; [C–H···π] 169, 158°) and 2) a [C–H···O] hydrogen bond between one of the corner

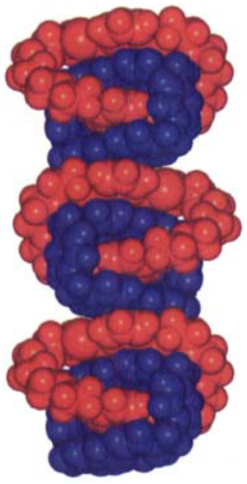

Figure 7. Packing diagram of the [2]catenane **23**·4PF$_6$ showing the donor–acceptor polar stack formed in the crystal.

methylene groups of the cyclophane and the oxygen atom next to sulfur in the polyether macrocycle ([C···O] 3.21 Å; [H···O] 2.37 Å; [C–H···O] 146°). The [2]catenanes pack to form polar stacks which are different from those observed for the other [2]catenanes in that previously, adjacent molecules within the stack were in register (they are related by a simple lattice translation), whereas here (Figure 7) the planes of alternate cyclophanes are twisted about the polar axis by approximately 61°. The intercatenane π–π stacking separation is 3.30 Å.

The X-ray analysis shows **24**·4PF$_6$ to adopt (Figure 8) a geometry in which the 1,5-dioxynaphthalene component of the macrocyclic polyether is positioned "inside" and sandwiched between the two bipyridinium units of the tetracationic cyclophane. The 1,5-dithiabenzene ring is positioned "outside". The $-OC_{10}H_6O-$ axis of the "inside" 1,5-dioxynaphthalene residue is inclined by 53° to the mean plane of the cyclophane, while the "outside" $-SC_6H_4S-$ vector is tilted by only 16°. The mean interplanar separations between the "inside" 1,5-dioxynaphthalene ring system and the "outside" and "inside" bipyridinium units are 3.47 and 3.36 Å, respectively. The interplanar distance between the "inside" bipyridinium unit and the "outside" 1,4-dihydroxybenzene ring is 3.48 Å. The only secondary stabilizing interactions in addition to the π–π stacking are the [C–H···π] interactions between the naphthalene C-4 and C-8 hydrogen atoms and the *p*-xylylene spacers of the cyclophane. There are no intracomponent [H···O] contacts of less than 2.5 Å. Packing of the molecules is the same as for **20**·4PF$_6$ with the formation of π–π polar stacks along their crystallographic C_2 axis. The intercatenane π–π stacking separation is 3.50 Å.

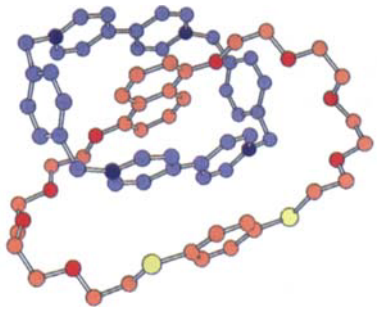

Figure 8. Geometry adopted by the [2]-catenane **24**·4PF$_6$ in the solid state.

The X-ray analysis of the complex formed between the tetracationic cyclophane **27**·4PF$_6$ and **17** (Figure 9; see also Figure 13) reveals the formation of a 1:2 complex, wherein one of the threads is inserted through the center of the cyclophane, while the other is sandwiched between the bipyridinium units of lattice-translated tetracations. Both independent 1,5-dioxynaphthalene units are positioned on crystallographic inversion centers, thus producing an overall superstructural arrangement that is markedly different (Figure 10) to that adopted by the "all-oxygen" analogue, where the 1,5-dioxynaphthalene and bipyridinium units all lie on a common C_2 axis. The pseudorotaxane portion of the 1:2 complex is stabilized by a combination of π–π stacking interactions with mean interplanar separations of 3.37 Å and [C–H···π] interactions ([H···π] 2.59 Å; [C–H···π] 150°), augmented by a strong pair of [C–H···O] hydrogen bonds ([C···O] 3.11 Å; [H···O] 2.23 Å; [C–H···O] 150°) between one of the α-pyridinium hydrogen atoms and the second oxygen (from the 1,5-dioxynaphthalene unit) atom of the complexed substrate. The 2:1 complexes form (Figure 11) an extended stack with the 1,5-dioxynaphthalene ring sandwiched between adjacent tetracations and overlaying just one pyridinium ring in each cyclophane with a mean interplanar separation of 3.28 Å in each case.

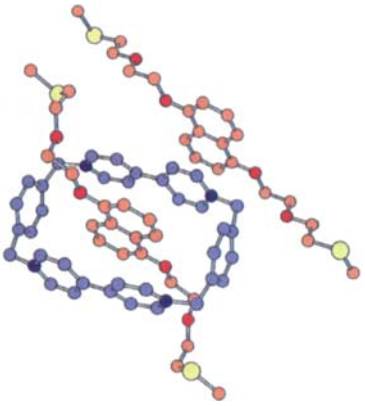

Figure 9. Geometry adopted by the complex formed between the π electron rich compound **17** and the tetracationic cyclophane **27**·4PF$_6$ in the solid state.

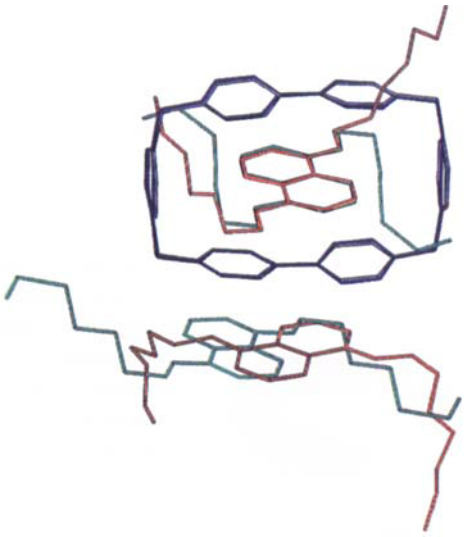

Figure 10. Comparison between the geometries adopted by the complexes formed by the tetracationic cyclophane **27**·4PF$_6$ (blue) with **17** (orange) and the "all-oxygen" analogue **15** (green) in the solid state.

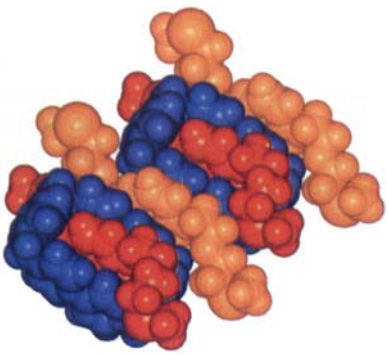

Figure 11. Packing diagram of the complex formed between the π electron rich compound **17** and the tetracationic cyclophane **27**·4PF$_6$ showing the donor–acceptor polar stack formed in the crystal.

0947-6539/97/0305-0776 $ 17.50+.50/0 Chem. Eur. J. 1997, 3, No. 5

The structures of the other two [2]pseudorotaxanes **14/27**·4PF_6 and **16/27**·4PF_6 were investigated, but were found to have nonstoichiometric disordered structures, wherein the tetracationic cyclophane components in each case form an orderly array, positioned about crystallographic symmetry centers and containing the naphthalene thread components at their centers. Because the combined lengths of the two thioether chains in each case is significantly longer than the separations between the cyclophane centers, the termini of the chains in one [2]pseudorotaxane overlay the region that would be occupied by an adjacent [2]pseudorotaxane if all the cyclophanes were simultaneously threaded. The apparent superstructure in each case—because of the crystallographic symmetry—simulates a pseudopolyrotaxane. A situation analogous to this one has been discussed previously by us.[9] As a consequence of our inability to unravel the multiple superimposed images, we are only reporting the unit cells and space groups for these two complexes.[10]

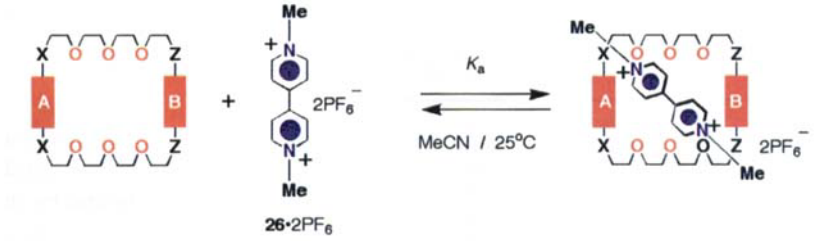

Macrocycle	X	Z	A	B	Complex
4	S	S	HQ	HQ	**4/26**·2PF_6
5	S	S	NP	NP	**5/26**·2PF_6
10	S	O	NP	NP	**10/26**·2PF_6
11	S	O	NP	HQ	**11/26**·2PF_6
12	S	O	HQ	NP	**12/26**·2PF_6
13	S	O	HQ	HQ	**13/26**·2PF_6
27	O	O	HQ	HQ	**27/26**·2PF_6
28	O	O	NP	NP	**28/26**·2PF_6
29	O	O	HQ	NP	**29/26**·2PF_6

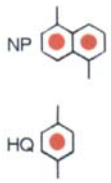

Figure 12. Complexation of the bis(hexafluorophosphate) salt **26**·4PF_6 by the π electron rich macrocycles **4**, **5**, and **10**–**13** (the "all-oxygen" analogues are also shown).

Association Constants: On mixing any of the π electron rich macrocyclic hosts **4**, **5**, and **10**–**13** with equimolar amounts of the π electron deficient bis(hexafluorophosphate) guest **26**·2PF_6 in MeCN, a red color develops as a result of charge-transfer interactions between the complementary aromatic units of host and guest, indicating the formation (Figure 12) of a complex in solution. The ^{1}H NMR spectra of equimolar mixtures of host and guest recorded in CD_3CN at 25 °C (Table 1) reveal changes in the chemical shift values of the hydrogen atoms attached to the aromatic units of the host and of the hydrogen atoms located in the α- and β-positions with respect to the nitrogen atoms on the bipyridinium units of the guest, compared with the values observed for "free" host and guest. Consistently, fast atom bombardment mass spectrometric (FABMS) analysis of the complexes (Table 2) reveals peaks at m/z values for $[M - PF_6]^+$ and $[M - 2PF_6]^+$, corresponding to the loss of

Table 1. Chemical shifts [δ values (Δδ values)] for the 1:1 complexes [a] **4/26**·2PF_6, **5/26**·2PF_6, and **10/26**·2PF_6–**13/26**·2PF_6 and reference compounds in CD_3CN at 25 °C.

Compound	Charged Component α-CH	Charged Component β-CH		Neutral Component H-4/H-8	Neutral Component H-3/H-7	Neutral Component H-2/H-6	Neutral Component -C_6H_4-
26·2PF_6	8.83	8.35					
4			SC_6H_4S				7.26
4/26·2PF_6	8.83	8.34					7.25
	(0.00)	(−0.01)					(−0.01)
5 [b]			$SC_{10}H_6S$	8.22	7.34	7.55	
5/26·2PF_6 [b]	8.81	8.28		8.15	7.33	7.51	
	(−0.02)	(−0.07)		(−0.07)	(−0.01)	(−0.04)	
10			$SC_{10}H_6S$	8.13	7.34	7.47	
			$OC_{10}H_6O$	7.70	7.18	6.72	
10/26·2PF_6	8.70	7.95	$SC_{10}H_6S$	7.88	7.29	7.33	
	(−0.13)	(−0.40)		(−0.25)	(−0.05)	(−0.14)	
			$OC_{10}H_6O$	7.55	7.15	6.65	
				(−0.15)	(−0.03)	(−0.07)	
11			$SC_{10}H_6S$	8.22	7.45	7.60	
			OC_6H_4O				6.64
11/26·2PF_6	8.78	8.18	$SC_{10}H_6S$	8.10	7.42	7.52	
	(−0.05)	(−0.17)		(−0.12)	(−0.03)	(−0.08)	
			OC_6H_4O				6.56
							(−0.08)
12			SC_6H_4S				7.05
			$OC_{10}H_6O$	7.79	7.32	6.89	
12/26·2PF_6	8.78	8.16	SC_6H_4S				6.94
	(−0.05)	(−0.19)					(−0.11)
			$OC_{10}H_6O$	7.68	7.28	6.82	
				(−0.11)	(−0.04)	(−0.07)	
13			SC_6H_4S				7.22
			OC_6H_4O				6.80
13/26·2PF_6	8.83	8.28	SC_6H_4S				7.15
	(0.00)	(−0.07)					(−0.07)
			OC_6H_4O				6.75
							(−0.05)

[a] The concentration of the components was 5 mM. [b] As a result of the low solubility of **5**, the solvent used was CD_3CN/CD_2Cl_2 (7:3, v/v).

  0947-6539/97/0305-0777 $ 17.50+.50/0

Table 2. FABMS data for the 1:1 complexes **4**/**26**·2PF$_6$, **5**/**26**·2PF$_6$, **10**/**26**·2PF$_6$–**13**/**26**·2PF$_6$, **15**/**27**·4PF$_6$, and **16**/**27**·4PF$_6$.

Complex	$[M]^+$ [a]	$[M-PF_6]^+$	$[M-2PF_6]^+$
4/**26**·2PF$_6$	(1076)	931	(786)
5/**26**·2PF$_6$	(1176)	1031	886
10/**26**·2PF$_6$	(1144)	999	854
11/**26**·2PF$_6$	1094	949	804
12/**26**·2PF$_6$	(1094)	949	804
13/**26**·2PF$_6$	1044	899	754
15/**27**·4PF$_6$	(1464)	(1319)	1174
16/**27**·4PF$_6$	(1496)	(1351)	1206

[a] "Molecular weight" of the 1:1 complex; the values in parentheses were not observed.

one and two hexafluorphosphate counterions, respectively. The association constants K_a for the resulting complexes (Table 3) were determined in MeCN at 25 °C by absorption UV/Vis spectrophotometric titration[11] at the wavelength λ_{max} corresponding to the maximum of the charge-transfer band associated with

Table 3. Association constants (K_a) and free energies of complexation ($-\Delta G^\circ$) for the 1:1 complexes formed by the π electron rich macrocycles **4**, **5**, and **10**–**13** and the bis(hexafluorophosphate) salt **26**·2PF$_6$ in MeCN at 25 °C.

Complex	K_a (M^{-1}) [a]	$-\Delta G^\circ$ (kcal mol^{-1}) [b]	λ_{max} (nm)
4/**26**·2PF$_6$	7 [c]	1.2	471
5/**26**·2PF$_6$	17 [d]	1.7	491
10/**26**·2PF$_6$	79	2.6	482
11/**26**·2PF$_6$	40	2.2	456
12/**26**·2PF$_6$	59	2.4	477
13/**26**·2PF$_6$	35	2.1	466

[a] The K_a values were determined by absorption UV/Vis spectrophotometric titration at the wavelength λ_{max} associated with the charge-transfer band of the complex (percentage error ≤ 14%). [b] Free energy of complexation (percentage error ≤ 17%). [c] Determined by ^{1}H NMR spectroscopy employing the continuous variation method. [d] Determined in MeCN/CH_2Cl_2 (7:3, *v*/*v*) as a result of the low solubility of **5**.

the complexes. The resulting values of K_a range from 7 to 79 M^{-1} and are significantly lower than those determined[12] in the case of the analogous "all-oxygen" macrocycles ($K_a > 700\,M^{-1}$). In the case of the macrocycle **2**, the K_a value is too low to be determined—an observation that is consistent with the very low efficiency of the corresponding catenation (see above). These observations show that the presence of sulfur atoms along the polythioether chains has a depressive influence upon the molecular recognition event. Presumably, in the case of **4**, **5**, and **10**–**13**—incorporating sulfur atoms directly attached to the aromatic units—the π–π stacking contribution to the binding energy is diminished, while in **2**—where the sulfur atoms are located well away from the aromatic units—it is the hydrogen bonding contribution that is reduced.

The higher stabilities of the complexes formed by **26**·4PF$_6$ and the "all-oxygen" π electron rich macrocycles contrast with the similar—in some instances even higher—yields associated with the catenations in the case of some of the sulfur-containing macrocycles (see above). The high efficiencies associated with these self-assembly processes could just possibly be a result of neighboring group participations of the sulfur atoms in the ring closure reaction (Scheme 6), leading to the formation of sulfonium intermediates.

The acyclic π electron rich guests **14**–**17** (Figure 13) are bound by the tetracationic host **27**·4PF$_6$, as indicated by the appearance of a purple color when equimolar amounts of host and guest are mixed in MeCN. Accordingly, the ^{1}H NMR spectra of equimolar mixtures of the host and guest recorded in CD_3CN at 25 °C (Table 4) show significant changes in the chemical shifts of the protons attached to the aromatic units of the guests and of the protons in the α- and β-positions with respect to the nitrogen atoms on the bipyridinium units of the host. Consistently, FABMS analysis of **15**/**27**·4PF$_6$ and **16**/**27**·4PF$_6$ (Table 2) revealed peaks at *m*/*z* values for $[M-2PF_6]^+$, corresponding to the loss of two hexafluorophosphate counterions. The association constants of the corresponding complexes (Table 5) were determined by absorption UV/Vis spectrophotometric titration at the wavelength corresponding to the maximum (λ_{max}) of the charge-transfer band of the complexes. The presence, as well as the location, of the sulfur atoms along the polythioether chains of the guests have a pronounced effect on the stabilities of the complexes. A very low value of K_a ($184\,M^{-1}$) was obtained in the case of the guest **16**, which incorporates one sulfur atom in the central positions of both of its two polythioether chains. Relocating the sulfur atom in either of the other two positions available along the polyether chains results in enhancement of the K_a values, which increase to 1010 and $1430\,M^{-1}$ for **14** and **17**, respectively. In contrast, a much higher value for K_a ($> 5000\,M^{-1}$) has been determined[13] for the "all-oxygen" compound **15**, as in the case of the 1:1 complexes formed by macrocyclic polyethers and **26**·4PF$_6$.

^{1}H NMR Spectroscopy: The chemical shifts associated with protons (other than the OCH_2 and SCH_2 protons) in the [2]catenanes **20**·4PF$_6$–**25**·4PF$_6$ are listed in Table 6. In all cases, the resonances of protons in the α- and β-positions with respect to the nitrogen atoms on the bipyridinium units of the tetracationic component are shifted with respect to those of the tetracationic cyclophane in its "free" form. Similarly, the resonances associated with the protons attached to the aromatic units of the π electron rich macrocyclic components are shifted significant-

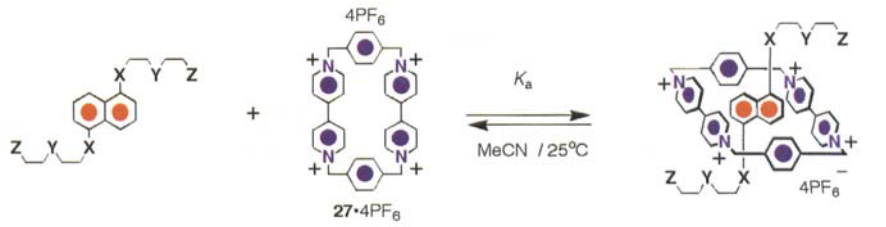

Compound	X	Y	Z	Complex
14	S	O	OMe	**14**/**27**·4PF$_6$
15	O	O	OMe	**15**/**27**·4PF$_6$
16	O	S	OMe	**16**/**27**·4PF$_6$
17	O	O	SMe	**17**/**27**·4PF$_6$

Figure 13. Complexation of the π electron rich acyclic compounds **14**–**17** by the tetracationic cyclophane **27**·4PF$_6$.

0947-6539/97/0305-0778 $ 17.50+.50/0 Chem. Eur. J. 1997, 3, No. 5

Table 4. Chemical shifts [δ values ($\Delta\delta$ values)] [a] for the 1:1 complexes [b] **14**/**27**·4PF$_6$–**17**/**27**·4PF$_6$ and reference compounds in CD_3CN at 25 °C.

Compound	Charged Component α-CH	β-CH	C_6H_4	CH_3N^+	Neutral Component H-4/H-8	H-3/H-7	H-2/H-6
27·4PF$_6$	8.86	8.16	7.52	5.74			
14					8.30	7.51	7.67
14/**27**·4PF$_6$	8.82	7.51	7.86	5.73		6.62	7.05
	(−0.04)	(−0.65)	(+0.34)	(−0.01)		(−0.89)	(−0.62)
15					7.79	7.38	6.94
15/**27**·4PF$_6$	8.95/8.67	7.34	7.98	5.71		6.06	6.33
	(+0.09/−0.19)	(−0.82)	(+0.46)	(−0.03)		(−1.32)	(−0.61)
16					7.79	7.38	6.95
16/**27**·4PF$_6$	8.81	7.81	7.72	5.74		6.89	6.71
	(−0.05)	(−0.35)	(+0.20)	(0.00)		(−0.49)	(−0.24)
17					7.80	7.38	6.94
17/**27**·4PF$_6$	8.81	7.47	7.92	5.75		6.46	
	(−0.05)	(−0.69)	(+0.40)	(+0.01)		(−0.92)	

[a] All the signals of the complexes are broad at 25 °C and the resonances associated with the hydrogen atoms H-4/H-8 in the 4- and 8-positions on the 1,5-disubstituted naphthalene units are not detectable. [b] The concentration of the components was 5 mM.

Table 5. Association constants (K_a) and free energies of complexation ($-\Delta G^\circ$) for the 1:1 complexes formed between tetracationic cyclophane **27**·4PF$_6$ and the π electron rich acyclic compounds **14**–**17** in MeCN at 25 °C.

Complex	K_a (M^{-1}) [a]	$-\Delta G^\circ$ (kcal mol^{-1}) [b]	λ_{max} (nm)
14/**27**·4PF$_6$	1010	4.1	541
15/**27**·4PF$_6$	>5000 [c]	>5	527
16/**27**·4PF$_6$	184	3.1	532
17/**27**·4PF$_6$	1430	4.3	527

[a] The K_a values were determined by absorption UV/Vis spectrophotometric titration at the wavelenght λ_{max} of the charge transfer band of the complex (percentage error ≤ 3%). [b] Free Energy of complexation (percentage error ≤ 6%). [c] Literature value (ref. [13]).

ly—up to ca. 6 ppm for the aromatic units residing "inside" the tetracationic cyclophane component.

The [2]catenanes **22**·4PF$_6$ and **23**·4PF$_6$ incorporate different π electron rich macrocyclic components. As a result, their ^{1}H NMR spectra show the existence of two translational isomers in solution (Figure 14). In the case of **22**·4PF$_6$, the 1,5-dithianaphthalene unit resides preferentially "inside" the cavity of the tetracationic cyclophane at low temperatures and, at −30 °C, the ratio between the two translational isomers **22a**·4PF$_6$ and **22b**·4PF$_6$ is 60:40. Raising the temperature up to +30 °C results in an increase of the population of the translational isomer **22b**·4PF$_6$, with the 1,5-dioxynaphthalene unit "inside", to a ratio of 55:45 in its favor. A more dramatic temperature dependence is observed in the case of **23**·4PF$_6$, where the ratio between **23a**·4PF$_6$ and **23b**·4PF$_6$ varies from 70:30 to 30:70 over the same range of temperatures. In contrast, only the translational isomer bearing the 1,4-dithiabenzene "outside" is observed for the [2]catenanes **24**·4PF$_6$—consistent with the geometry adopted in the solid state (see above)—and **25**·4PF$_6$.

The dynamic processes illustrated schematically in Figures 15–17 are associated with the [2]catenanes **20**·4PF$_6$–**25**·4PF$_6$ in solution. Process I (Figure 15) involves the circumrotation of the macrocyclic polythioether component through the cavity of the tetracationic cyclophane component. Process II (Figure 15) involves the circumrotation of the tetracationic cyclophane component through the cavity of the macrocyclic polythioether component. Process III (Figure 16) involves the "rocking" of the aromatic unit located "inside" the cavity of the π electron defi-

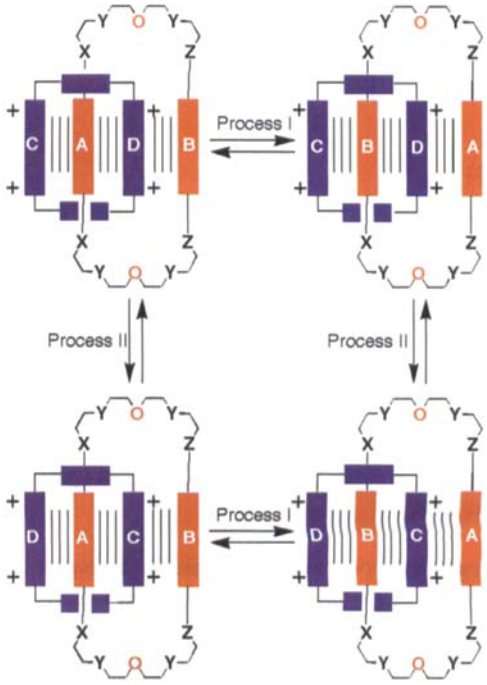

Figure 15. Dynamic Processes I and II associated with the [2]catenanes in solution.

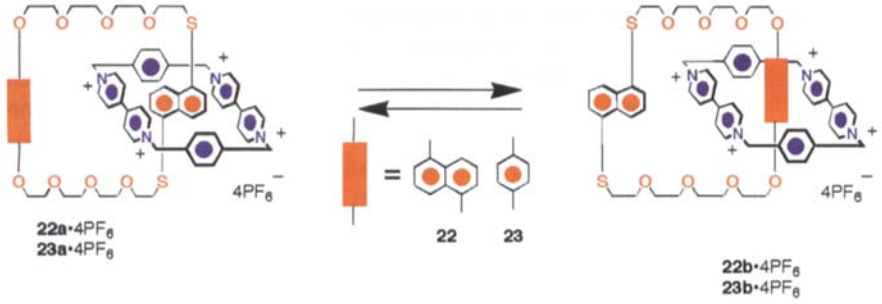

Figure 14. Translational isomers associated with the [2]catenanes **22**·4PF$_6$ and **23**·4PF$_6$.

Table 6. Chemical shifts [δ values ($\Delta\delta$ values)] for the [2]catenanes **20**·4PF$_6$–**25**·4PF$_6$ in CD$_3$CN at 20–25 °C [a].

Compound	Charged Component α-CH	β-CH	-C$_6$H$_4$-	CH$_2$N		Neutral Component H-4/8	H-3/7	H-2/6	OC$_6$H$_4$O
4					SC$_6$H$_4$S				7.26
20·4PF$_6$	8.90	7.81	7.81	5.72	inside SC$_6$H$_4$S				5.47 [c]
	(+0.04)	(−0.35)	(+0.29)	(−0.02)					(−1.79)
					alongside SC$_6$H$_4$S				5.47 [d]
									(−1.79)
5					SC$_{10}$H$_6$S	8.22	7.55	7.34	
21·4PF$_6$ [b]	8.58	6.79	7.92	5.72	inside SC$_{10}$H$_6$S	2.05	5.87	6.40	
	(−0.28)	(−1.37)	(+0.40)	(−0.02)		(−6.17)	(−1.68)	(−0.94)	
					alongside SC$_{10}$H$_6$S	7.24	7.08	6.64	
						(−0.98)	(−0.47)	(−0.70)	
10					SC$_{10}$H$_6$S	8.13	7.34	7.47	
					OC$_{10}$H$_6$O	7.70	7.18	6.72	
22·4PF$_6$	8.63	6.81	7.97	5.74	inside SC$_{10}$H$_6$S	2.21	5.94	6.49	
	(−0.23)	(−1.35)	(+0.45)	(0.00)		(−5.92)	(−1.40)	(−0.98)	
					alongside SC$_{10}$H$_6$S	7.41	7.18	6.87	
						(−0.72)	(−0.16)	(−0.60)	
					inside OC$_{10}$H$_6$O	2.27	5.83	6.09	
						(−5.43)	(−1.35)	(−0.63)	
					alongside OC$_{10}$H$_6$O	7.18	7.09	6.29	
						(−0.52)	(−0.09)	(−0.43)	
11					SC$_{10}$H$_6$S	8.22	7.45	7.60	
					OC$_6$H$_4$O				6.64
23·4PF$_6$	8.75	7.26	7.87	5.70	inside SC$_{10}$H$_6$S	2.31	6.04	6.58	
	(−0.11)	(−0.90)	(+0.35)	(−0.04)		(−5.92)	(−1.41)	(−1.02)	
					alongside SC$_{10}$H$_6$S	7.55	7.26	6.94	
						(−0.67)	(−0.19)	(−0.66)	
					inside OC$_6$H$_4$O				3.36
									(−3.28)
					alongside OC$_6$H$_4$O				6.04
									(−0.60)
12					SC$_6$H$_4$S				7.05
					OC$_{10}$H$_6$O	7.79	7.32	6.89	
24·4PF$_6$	8.76	7.14	8.02	5.75	alongside SC$_6$H$_4$S				6.53
	(−0.10)	(−1.02)	(+0.50)	(+0.01)					(−0.52)
					inside OC$_{10}$H$_6$O	2.42	5.94	6.21	
						(−5.37)	(−1.38)	(−0.68)	
13					SC$_6$H$_4$S				7.22
					OC$_6$H$_4$O				6.80
25·4PF$_6$	8.89	7.66	7.81	5.70	alongside SC$_6$H$_4$S				6.63
	(+0.03)	(−0.50)	(+0.29)	(−0.04)					(−0.59)
					inside OC$_6$H$_4$O				3.52
									(−3.28)

[a] The concentration of the compounds was 10 mM. [b] The values reported are determined at the centers of the multiplets. [c] Recorded at −35 °C. [d] Value determined at 70 °C.

cient macrocyclic component with respect to its mean plane. Process IV (Figure 17) is associated with the [2]catenanes incorporating a 1,5-disubstituted naphthalene ring system "inside" and involves 1) extrusion of the naphthalene unit from the cavity of the tetracationic cyclophane, 2) a rotation of the 1,5-disubstituted naphthalene and/or the bipyridinium unit(s), and 3) reinsertion of the naphthalene ring system "inside" the cavity of the tetracationic cyclophane. The free energy barriers (Table 7) associated with the dynamic Processes I–IV were determined by variable-temperature ^{1}H NMR spectroscopy employing the approximate coalescence method.[14]

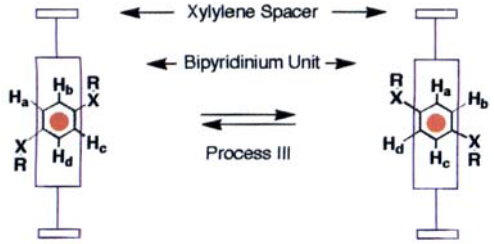

Figure 16. Dynamic Process III associated with the [2]catenanes in solution.

In the case of the [2]catenane **20**·4PF$_6$, incorporating two 1,4-dithiabenzene rings within its π electron rich macrocyclic component, weak intracomponent interactions exist, as suggested by 1) the low yield of its self-assembly process and 2) the low K_a value for the complexation of **26**·2PF$_6$ by the π electron rich macrocycle **4**. As a result, only Process I can be "frozen out" on the ^{1}H NMR timescale at 193 K in (CD$_3$)$_2$CO—the other processes are too fast, even at this very low temperature. By employing the approximate coalescence method (Table 7), a value of 12.2 kcal mol^{-1} was derived for the free energy of activation $\Delta G_c^{\ddagger}$ at a coalescence temperature T_c of 283 K in (CD$_3$)$_2$CO (cf., $\Delta G_c^{\ddagger}$ = 15.6 kcal mol^{-1} at T_c = 354 K for the "all-oxygen" analogue **1**·4PF$_6$ in CD$_3$CN[4]).

0947-6539/97/0305-0780 $ 17.50+.50/0 Chem. Eur. J. 1997, 3, No. 5

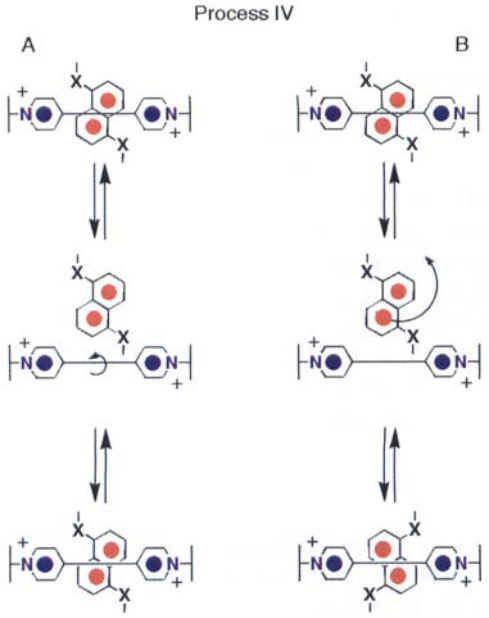

Figure 17. Dynamic Process IV associated with the [2]catenanes containing 1,5-disubstituted naphthalene units in solution.

In the case of **21**·4PF$_6$, Processes I, II, and IV are slow on the ^{1}H NMR timescale at temperatures just above the freezing point of $(CD_3)_2CO$ (i.e., at the lowest possible practical temperature limit). As a result, the kinetic and thermodynamic parameters associated with Processes I, II, and IV were determined (Table 7), once again, by the approximate coalescence method. Values for $\Delta G_c^{\ddagger}$ significantly lower (ca. 1.5 kcal mol^{-1}) than those obtained in the case of the "all-oxygen" analogue were determined.[8]

Two translational isomers (Figure 14) exist in solution in the case of the [2]catenane **22**·4PF$_6$. The ^{1}H NMR spectra of **22**·4PF$_6$, recorded in $(CD_3)_2CO$ below 228 K, reveals four doublets for the protons in the α-positions with respect to the nitrogen atoms on the bipyridinium units of the tetracationic cyclophane component in the case of each translational isomer. Free energy barriers of 11.8 and 10.6 kcal mol^{-1} were determined in $(CD_3)_2CO$ at coalescence temperatures of 253 and 228 K, respectively, for isomers **22a**·4PF$_6$ and **22b**·4PF$_6$, respectively, from the coalescence of the four doublets into two in each case. Further coalescence of the two doublets into one doublet for each isomer provided an opportunity to determine the $\Delta G_c^{\ddagger}$ values for Process IV. These values correspond to 14.9 and 16.1 kcal mol^{-1} at coalescence temperatures of 323 and 343 K, respectively, for isomers **22a**·4PF$_6$ and **22b**·4PF$_6$, respectively, in CD_3CN. In addition, by employing the protons attached to the 2- and 6-positions of one of the two 1,5-disubstituted naphthalene ring systems as probes, the free energy barriers for the interconversion of the major into the minor isomer (Process I a) and for the interconversion of the minor into the major isomer (Process I b) were calculated to be 15.3 and 15.5 kcal mol^{-1}, respectively.[15]

Since only the translational isomer with the 1,5-dioxynaphthalene unit located "inside" the cavity of the tetracationic cyclophane is observed, the dynamic behavior of the [2]catenane **24**·4PF$_6$ is relatively simple. The $\Delta G_c^{\ddagger}$ values associated with Processes II and IV (Table 7) were measured in $(CD_3)_2CO$ and in CD_3CN, respectively, from the coalescence of the resonances of the protons attached to the *p*-xylylene spacers of the tetracationic cyclophane. Below the coalescence temperature (213 K), Processes II and IV are slow on the ^{1}H NMR timescale, and the four protons of each *p*-xylylene unit are inequivalent, giving rise to two independent AB systems. In contrast, above 213 K, Process II becomes fast on the ^{1}H NMR timescale and only two singlets are observed for the *p*-xylylene protons. Coalescence of these two singlets to give only one signal occurs by further warming of a CD_3CN solution of **24**·4PF$_6$, as a result of increasing the rate of Process IV, which becomes fast on the ^{1}H NMR timescale.

Also, only one translational isomer exists for the [2]catenane **25**·4PF$_6$ in solution. The $\Delta G_c^{\ddagger}$ value for Process III (Table 7) was determined in $(CD_3)_2CO$ from the coalescence of the two doublets observed at temperatures lower than T_c (228 K) for the resonances associated with the hydroquinone ring protons into only one singlet at higher temperatures. The coalescence of the two doublets—observed for the protons in the α-positions with respect to the nitrogen atoms on the bipyridinium units of the tetracationic cyclophane—above a T_c of 228 K into only one doublet provided the opportunity to determine a $\Delta G_c^{\ddagger}$ value of 10.8 kcal mol^{-1} for Process II in $(CD_3)_2CO$.

Table 7. Kinetic data associated with the dynamic processes occurring in solution within the [2]Catenanes **20**·4PF$_6$-**25**·4PF$_6$.

[2]Catenane	Probe	Solvent	$\Delta\nu$ [a] (Hz)	k_c [b] (s^{-1})	T_c [c] (K)	$\Delta G_c^{\ddagger}$ [d] (kcal mol^{-1})	Process
20·4PF$_6$	SC_6H_4S	$(CD_3)_2CO$	988	2200	283	12.2	I
21·4PF$_6$	naphthalene H2/6	$(CD_3)_2CO$	53	118	313	15.4	I
	α-bipyridinium	$(CD_3)_2CO$	198	440	221	10.1	II
	α-bipyridinium	$(CD_3)_2CO$	172	382	310	14.5	IV
22·4PF$_6$	naphthalene H2/6	CD_3CN	78	309	336	15.3	I a
	naphthalene H2/6	CD_3CN	78	181	336	15.5	I b
	α-bipyridinium	$(CD_3)_2CO$	160	355	253	11.8	II a
	α-bipyridinium	$(CD_3)_2CO$	135	300	228	10.6	II b
	α-bipyridinium	CD_3CN	237	526	323	14.9	IV a
	α-bipyridinium	CD_3CN	174	387	343	16.1	IV b
24·4PF$_6$	*p*-xylylene	$(CD_3)_2CO$	50	111	213	10.3	II
	p-xylylene	CD_3CN	74	164	328	15.9	IV
25·4PF$_6$	α-pyridinium	$(CD_3)_2CO$	57	127	223	10.8	II
	OC_6H_4O	$(CD_3)_2CO$	1368	3037	228	9.6	III

[a] Frequency difference (percentage error ≤ 0.2%). [b] Rate constant at the coalescence temperature (percentage error ≤ 0.2%). [c] Coalescence temperature (percentage error ≤ 2.0%). [d] Free energy barrier at the coalescence temperature (percentage error ≤ 2.0%).

Electrochemistry: Cyclic voltammetry of the tetracationic cyclophane **27**·4PF$_6$[4] shows two reversible reduction processes with half-wave potentials of −283 and −708 mV corresponding to two-electron reductions of the couples [bipyridinium]$^{2+}$/[bipyridinium]$^{+}$ and [bipyridinium]$^{+}$/[bipyridinium], respectively. These observations suggest that the two bipyridinium units of the tetracationic cyclophane **27**·4PF$_6$ are reduced simultaneously as a result of two consecutive additions of two electrons. In contrast, when the tetracationic cyclophane is mechanically interlocked within a [2]catenane, the two bipyridinium units are no longer equivalent. The bipyridinium unit located "inside" the cavity of the π electron rich macrocyclic polyether is reduced at more negative potentials as a result of the stabilizing π−π stacking interactions with the two π electron rich aromatic units incorporated within the macrocyclic polyether. Thus, cyclic voltammetry of the [2]catenanes **21**·4PF$_6$–**25**·4PF$_6$ (Table 8) shows three reversible reduction processes. The first two processes are monoelectronic reductions of the "outside" and "inside" bipyridinium units, respectively, while the third process is a two-electron addition corresponding to the almost simultaneous reduction of the two bipyridinium radical cations. Presumably, once both bipyridinium units are monoelectronically reduced their acceptor character is diminished and "outside" and "inside" units are no longer distinguishable and so are reduced almost simultaneously with the second pair of electrons. In contrast, only two reduction potentials are evident in the case of the [2]catenane **20**·4PF$_6$, as a result of the almost simultaneous monoelectronic reduction of "outside" and "inside" bipyridinium units. Comparison of the reduction potentials of the [2]catenanes **20**·4PF$_6$–**25**·4PF$_6$ with those determined for their "all-oxygen" analogues **1**·4PF$_6$, **28**·4PF$_6$, and **29**·4PF$_6$[4, 8, 16] revealed significant differences in the E_1' values, as a result of a diminished degree of π-donation associated with the dithioarene units. This observation is consistent with the depressive effect observed (see above) in the K_a values on introducing sulfur in place of oxygen atoms in the macrocycles.

Table 8. Reduction potentials (vs. SCE) associated with the [2]catenanes **20**·4PF$_6$–**25**·4PF$_6$ and their "all-oxygen" analogues **1**·4PF$_6$, **28**·4PF$_6$, and **29**·4PF$_6$ in a 0.1 M solution of ^{t}BuN·PF$_6$ in MeCN.

Compound	XC_nH_mX/XC_nH_mX [a]	E_1 (mV)	E_1' (mV)	E_2 (mV)
1·4PF$_6$ [b]	OC_6H_4O/OC_6H_4O	−310	−437	−845
25·4PF$_6$	OC_6H_4O/SC_6H_4S	−311	−401	−849
20·4PF$_6$	SC_6H_4S/SC_6H_4S	−300	− [c]	−842
28·4PF$_6$ [d]	$OC_{10}H_5O/OC_{10}H_5O$	−354	−572	−861
22·4PF$_6$	$OC_{10}H_5O/SC_{10}H_5S$	−324	−488	−797
21·4PF$_6$	$SC_{10}H_5S/SC_{10}H_5S$	−336	−423	−782
29·4PF$_6$ [e]	$OC_6H_4O/OC_{10}H_5O$	−330	−460	−800
23·4PF$_6$	$OC_6H_4O/SC_{10}H_5S$	−308	−424	−815
24·4PF$_6$	$SC_6H_4S/OC_{10}H_5O$	−325	−389	−859

[a] Aromatic units incorporated within the π electron rich macrocyclic components of the [2]catenanes. [b] Literature values (ref. [4]). [c] The reduction potentials E_1 and E_1' cannot be distinghuished. [d] Literature values (ref. [8]). [e] Literature values (ref. [15]).

Conclusions

A series of 1:1 complexes possessing pseudorotaxane-like geometries have been self-assembled in solution and in the solid state as a result of cooperative noncovalent bonding interactions such as 1) π−π stacking, 2) [C−H···O] hydrogen bonding, and 3) [C−H···π] edge-to-face interactions. These complexes incorporate either π electron rich macrocyclic polythioether hosts and the bipyridinium-based salt, paraquat, as guest, or π electron rich acyclic polythioether guests and the bipyridinium-based cyclophane, cyclobis(paraquat-*p*-phenylene), as host. The π electron rich polythioether macrocycles were employed to self-assemble a range of [2]catenanes incorporating cyclobis(paraquat-*p*-phenylene) as the second ring component. Surprisingly—despite the lower association constants for the 1:1 complexes in comparison with the analogous "all-oxygen" compounds—the self-assembly of these [2]catenanes are amongst the most efficient catenations reported in the literature. Careful examination of the mechanism of catenane formation with the aid of computational methods may provide the answer to such apparently contradictory results. Single crystal X-ray analyses of the [2]catenanes revealed the presence of only one of the two possible translational isomers associated with the [2]catenanes incorporating different π electron rich aromatic ring systems in their macrocyclic polythioether components. In particular, the dioxyarene ring systems reside "inside" the cavity of the tetracationic component in preference to the dithiarene ring systems. When 1,5-disubstituted naphthalene and 1,4-disubstituted benzene ring systems with the same subsituents are incorporated within the π electron rich macrocycle, the former is preferentially located "inside". Thus, the following "selection rule" exists in the solid state: $OC_{10}H_6O > OC_6H_4O > SC_{10}H_6S > SC_6H_4S$. A similar selectivity is observed in solution for the [2]catenanes **24**·4PF$_6$ and **25**·4PF$_6$ incorporating exclusively $OC_{10}H_6O$ "inside" and SC_6H_4S "outside", and OC_6H_4O "inside" and SC_6H_4S "outside", respectively. In contrast, a temperature dependence of the equilibrium between the translational isomers associated with **22**·4PF$_6$ and **23**·4PF$_6$ is observed: these [2]catenanes can be regarded as temperature-responsive molecular switches. The dynamic processes associated with the [2]catenanes in solution were investigated by variable-temperature ^{1}H NMR spectroscopy. The free energy barriers of these dynamic processes are lower than in the case of the "all-oxygen" analogues, presumably, as a result of the weaker intercomponent interactions. Consistently, cyclic voltammetric investigation of the [2]catenanes revealed redox potentials, for the reduction of the bipyridinium units incorporated within the catenanes, at values lower than in the case of the "all-oxygen" analogues, reflecting the lower π-donation ability of the dithioarene units.

Experimental Section

General Methods: Chemicals were purchased from Acros Organics, Aldrich, or TCI and used as received. Solvents were purified and dried according to methods described in the literature.[17] 1,4-Bis(2-bromoethoxy)benzene,[18] 1,5-naphthalenedithiol,[19] tetraethyleneglycol monotosylate,[2g] 1,5-bis(2-(2-tosyloxyethoxy)ethoxy)naphthalene,[2g] 1,5-bis(2-(2-(2-(2-tosyloxyethoxy)-ethoxy)ethoxy)ethoxy)naphthalene (**8**),[2g] 1,4-bis(2-(2-(2-(2-tosyloxyetho-

0947-6539/97/0305-0782 $ 17.50+.50/0 Chem. Eur. J. 1997, 3, No. 5

xy)ethoxy)ethoxy)ethoxy)benzene (**9**),[2d] 1,5-bis(2-(2-methoxyethoxy)-ethoxy)naphthalene (**15**),[13] and 1,4-bis[4-(4-pyridyl)pyridiniummethylene]-benzene bis(hexafluorophosphate) (**18**)[4] were all prepared according to literature procedures. Reactions under ultrahigh pressure were carried out in Teflon vessels using a custom-built ultrahigh pressure reactor manufactured by PSIKA Pressure Systems of Glossop, UK. Thin-layer chromatography (TLC) was carried out on aluminum sheets, precoated with silica gel 60F (Merck 5554). The plates were inspected with UV light. Column chromatography was carried out using silica gel 60F (Merck 9385, 230–400 mesh). Melting points were determined using a Reichert Thermovar apparatus and were not corrected. Low-resolution electron-impact mass spectra were recorded using a Hewlett Packard 5989A spectrometer operating at 70 eV. Fast atom bombardment mass spectra (FABMS) were recorded on a Kratos MS80 spectrometer operating at 8 keV using a xenon primary atom beam; the matrix used was 3-nitrobenzyl alcohol. High-resolution electron impact mass spectra were obtained using a Kratos MS 50 TC instrument operating at 70 eV. UV/Vis spectra were recorded on a Perkin-Elmer Lamda 2 using HPLC quality solvents. Nuclear magnetic resonance (NMR) spectra were recorded on Bruker WM 250, AC 300, or AMX 400 spectrometers, using the solvent or TMS as internal standard. All chemical shifts are quoted on the δ scale and the coupling constants J are given in Hertz (Hz). Microanalyses were performed by Analytical Labs (Lindbar, Germany).

4,10,21,27-Tetrathiabis-*p*-phenylene[34]crown-10 (2): A solution of 1,4-bis(2-bromoethoxy)benzene (3.24 g, 10.0 mmol) and 1,5-dimercapto-3-oxapentane (1.38 g, 10.0 mmol) in DMF (50 mL) was added during 24 h at a constant rate, with the aid of an infusion pump, to a stirred suspension of K_2CO_3 (8.28 g, 60.0 mmol) in DMF (300 mL) at 70 °C under a nitrogen atmosphere. After completion of the addition, heating and stirring were continued for an additional 24 h. The solution was cooled down to room temperature and the solvent was removed under reduced pressure. The residue was treated with CH_2Cl_2 (500 mL), washed with H_2O (3 × 500 mL) and dried ($MgSO_4$). After evaporation of the solvent in vacuo, the resulting oil was subjected to column chromatography (SiO_2, $MeCO_2Et/CH_2Cl_2$, 20:1) to afford the macrocyclic polythioethers **2** (150 mg, 5%) and **3** (930 mg, 31%); both compounds were crystallized from acetone. When the reaction was carried out with Cs_2CO_3 as the base, **2** and **3** were obtained in 7 and 46%, respectively.

2: m.p. 99 °C; EIMS: m/z 600 $[M]^+$; ^{1}H NMR ($CDCl_3$): δ = 6.78 (s, 8H), 4.06 (t, J = 6.7 Hz, 8H), 3.68 (t, J = 6.3 Hz, 8H), 2.90 (t, J = 6.7 Hz, 8H), 2.79 (t, J = 6.3 Hz, 8H); ^{13}C NMR ($CDCl_3$): δ = 152.8, 115.6, 71.4, 68.7, 32.2, 31.7; Anal. calcd for $C_{36}H_{44}O_6S_4$: C 56.0, H 6.71; found C 55.8, H 6.83.
3: m.p. 54 °C; EIMS: m/z 300 $[M]^+$; ^{1}H NMR ($CDCl_3$): δ = 6.97 (s, 4H), 4.30 (t, J = 6.3 Hz, 4H), 3.18 (t, J = 7.4 Hz, 4H), 2.78 (t, J = 6.3 Hz, 4H), 2.39 (t, J = 7.4 Hz, 4H); ^{13}C NMR ($CDCl_3$): δ = 152.0, 119.0, 70.9, 69.5, 30.2, 28.9.

1,13,18,30-Tetrathiabis-*p*-phenylene[34]crown-10 (4): A suspension of 1,11-dichloro-3,6,9-trioxaundecane (11.6 g, 50.0 mmol), 4-aminothiophenol (12.5 g, 100 mmol), and K_2CO_3 (13.8 g, 100 mmol) in dry MeCN (250 mL) was heated under reflux for 24 h under a nitrogen atmosphere. After cooling down to room temperature, the mixture was filtered, and the filtrate was evaporated in vacuo. Purification of the residue by column chromatography (SiO_2, $MeCO_2Et/CH_2Cl_2$, 3:7) gave 1,11-bis(4-aminophenylthio)-3,6,9-trioxaundecane as a pale yellow oil (15.10 g, 74%). ^{1}H NMR ($CDCl_3$): δ = 7.22 (d, J = 8 Hz, 4H), 6.59 (d, J = 8 Hz, 4H), 3.66 (s, 4H), 3.64-3.50 (m, 12H), 2.92 (t, J = 7 Hz, 4H); ^{13}C NMR ($CDCl_3$): δ = 145.8, 134.0, 122.7, 115.5, 70.4, 70.1, 70.0, 35.4.

The resulting bisamine (8.16 g, 20.0 mmol) was dissolved in aqueous HCl (50 mL, 6%) and cooled to 0 °C. A solution of $NaNO_2$ (3.04 g, 44.0 mmol) in H_2O (20 mL) was added slowly, while keeping the temperature below 5 °C. After stirring for another 15 min at 0 °C, the mixture was treated with aqueous NaOAc (10.0 g, 120 mmol in 30 mL) and the whole was added dropwise with stirring to a solution of $EtOCS_2K$ (12.8 g, 80.0 mmol) in H_2O (40 mL) at 80 °C. The mixture was stirred for a further 2 h at 80 °C and then diluted with H_2O (50 mL) and extracted with CH_2Cl_2 (3 × 200 mL). The combined extracts were dried (Mg_2SO_4) and evaporated to give a brown oil, which was dissolved in EtOH (300 mL). KOH (10 g, 180 mmol) was added and the ethanolic solution was heated under reflux for 3 h under a nitrogen atmosphere. The reaction mixture was acidified with aqueous HCl (250 mL, 15%) and extracted with CH_2Cl_2 (3 × 250 mL). After removal of the solvent under reduced pressure, the residue was subjected to column chromatography (SiO_2, $MeCO_2Et/CH_2Cl_2$, 1:9) to give 1,11-bis(4-mercaptophenylthio)-3,6,9-trioxaundecane as a pale yellow oil (2.28 g, 26%). ^{1}H NMR ($CDCl_3$): δ = 7.30–7.10 (2d, J = 8 Hz, 8H), 3.65–3.54 (m, 12H), 3.42 (s, 2H), 3.06 (t, J = 7 Hz, 4H); ^{13}C NMR ($CDCl_3$): δ = 133.4, 130.5, 130.0, 128.7, 70.6, 70.4, 69.9, 33.5.

A mixture of this bisthiol (1.11 g, 2.50 mmol) and 1,11-bis(tosyloxy)-3,6,9-trioxaundecane (1.26 g, 2.50 mmol) in DMF (50 mL) was added at a constant rate during 24 h to a stirred suspension of Cs_2CO_3 (4.89 g, 15.0 mmol) in DMF (300 mL) at 70 °C under a nitrogen atmosphere, and the reaction mixture was then stirred for another 24 h at 70 °C. After workup and column chromatography (SiO_2, $MeCO_2Et/CH_2Cl_2$, 1:19) according to the procedure described for **2**, the macrocycle **4** was obtained as a white solid (360 mg, 24%) and crystallized from CH_2Cl_2/Et_2O (271 mg, 18%). m.p. 74 °C; FABMS: m/z 600 $[M]^+$; ^{1}H NMR ($CDCl_3$): δ = 7.26 (s, 8H), 3.65 (t, J = 7 Hz, 8H), 3.61 (s, 16H), 3.08 (t, J = 7 Hz, 8H); ^{13}C NMR ($CDCl_3$): δ = 133.8, 130.0, 70.7, 70.4, 69.8, 33.2; Anal. calcd for $C_{28}H_{40}O_6S_4$: C 56.0 H 6.71; found C 55.8, H 6.51.

1,13,20,32-Tetrathiabis-1,5-naphtho[38]crown-10 (5):
Method A: A mixture of 1,5-naphthalenedithiol (2.88 g, 15.0 mmol) and 1,11-bis(tosyloxy)-3,6,9-trioxaundecane (7.54 g, 15.0 mmol) in DMF (50 mL) was added at a constant rate during 24 h to a stirred suspension of Cs_2CO_3 (14.7 g, 45.0 mmol) in DMF (500 mL) at 70 °C under a nitrogen atmosphere, and the reaction mixture was then stirred for another 12 h at 70 °C. After workup according to the procedure described for **2** and evaporation of the solvent, the residue was crystallized from Me_2CO to give the macrocycle **6** (2.13 g, 41%). The filtrate was subjected to column chromatography (SiO_2, $Et_2O/CH_2Cl_2/CH_3OH$, 68:30:2) to give **5** (380 mg, 7%), together with an additional amount of the ansa compound **6** (308 mg, 6%). Both compounds **5** and **6** were recrystallized from Me_2CO.

5: m.p. 98 °C; FABMS: m/z 700 $[M]^+$; ^{1}H NMR ($CDCl_3$): δ = 8.33 (d, J = 8 Hz, 4H), 7.59 (d, J = 7 Hz, 4H), 7.35 (m, 4H), 3.61 (t, J = 6.7 Hz, 8H), 3.57–3.48 (m, 16H), 3.10 (t, J = 6.7 Hz, 8H); ^{13}C NMR ($CDCl_3$): δ = 133.8, 133.7, 129.4, 125.9, 124.8, 70.7, 70.5, 69.7, 34.2; Anal. calcd for $C_{36}H_{44}O_6S_4$: C 61.7, H 6.33; found C 61.6, H 6.43.

6: m.p. 113 °C; EIMS: m/z 350 $[M]^+$; ^{1}H NMR ($CDCl_3$): δ = 8.63 (d, J = 8 Hz, 2H), 7.86 (d, J = 7 Hz, 2H), 7.49 (m, 2H), 3.67–3.50 (m, 4H), 3.14–2.95 (m, 8H), 2.86–2.75 (m, 4H); ^{13}C NMR ($CDCl_3$): δ = 135.4, 133.8, 133.6, 127.2, 125.8, 72.0, 70.4, 69.9, 36.0; Anal. calcd for $C_{18}H_{22}O_3S_2$: C 61.7, H 6.33; found C 61.6, H 6.40.

Method B: 1,5-Naphthalenedithiol (4.80 g, 25.0 mmol) and tetraethyleneglycol monotosylate (17.4 g, 50.0 mmol) were added to a suspension of K_2CO_3 (10.4 g, 75.0 mmol) in dry MeCN (200 mL), and the reaction mixture was refluxed for 4 d under a nitrogen atmosphere. The solvent was removed in vacuo and the residue was treated with CH_2Cl_2 (500 mL) and washed with H_2O (3 × 500 mL). The organic phase was dried ($MgSO_4$) and the solvent evaporated under reduced pressure to give 1,5-bis(2-(2-(2-(2-hydroxyethoxy)ethoxy)ethoxy)ethylthio)naphthalene as a yellow oil. This compound was dissolved in CH_2Cl_2 (100 mL) containing Et_3N (30.3 g, 300 mmol) and a catalytic amount of *p*-(dimethylamino)pyridine (122 mg, 1.00 mmol). Tosyl chloride (11.43 g, 60 mmol) in CH_2Cl_2 (100 mL) was added to this solution dropwise with stirring at 0 °C, and the whole was stirred overnight at room temperature. The reaction mixture was washed with aqueous HCl (100 mL, 2M) and H_2O (2 × 100 mL), dried ($MgSO_4$) and evaporated in vacuo. Purification of the residue by column chromatography (SiO_2, CH_2Cl_2/MeOH, 19:1) gave compound **7** as a pale yellow oil (13.7 g, 64%).

7: ^{1}H NMR ($CDCl_3$): δ = 8.36 (d, J = 8 Hz, 2H), 7.78 (d, J = 8 Hz, 4H), 7.65 (d, J = 7 Hz, 2H), 7.46 (m, 2H), 7.31 (d, J = 8 Hz 4H), 4.14 (t, J = 5 Hz, 4H), 3.66 (t, J = 5 Hz, 4H), 3.65 (t, J = 7 Hz, 4H), 3.54–3.60 (m, 16H), 3.16 (t, J = 7 Hz, 4H), 2.42 (s, 6H); ^{13}C NMR ($CDCl_3$): δ = 144.7, 133.8, 133.6, 132.9, 129.8, 129.0, 127.9, 125.9, 124.6, 70.7, 70.5 (2 signals), 70.3, 69.7, 69.2, 68.6, 33.8, 21.6.

Compound **7** (4.26 g, 5 mmol) and 1,5-naphthalenedithiol (0.96 g, 5 mmol) in DMF (50 mL) were added at a constant rate during 24 h to a stirred suspension of Cs_2CO_3 (4.90 g, 15 mmol) in DMF (300 mL) at 70 °C under a nitrogen atmosphere, and the reaction mixture was then stirred overnight at 70 °C. After workup and column chromatography (SiO_2, Et_2O/CH_2Cl_2/MeOH, 68:30:2) according to the general procedure described for **2**, the macrocycle **5** was obtained as a white solid (1.37 g, 39%) and crystallized from Me_2CO (853 mg, 24%).

1,32-Dithiabis-1,5-naphtho[38]crown-10 (10): A mixture of 1,5-naphthalenedithiol (0.96 g, 5.0 mmol) and **8** (4.1 g, 5.0 mmol) in DMF (50 mL) was added at a constant rate during 24 h to a stirred suspension of Cs_2CO_3 (4.90 g, 15.0 mmol) in DMF (300 mL) at 70 °C under a nitrogen atmosphere, and the reaction mixture was stirred overnight at 70 °C. After workup and column chromatography (SiO_2/Et_2O/CH_2Cl_2/MeOH, 68:30:2) according to the procedure described for **2**, the macrocycle **10** was obtained as a white solid (1.18 g, 35%) and crystallized from Me_2CO (866 mg, 26%). m.p. 92 °C; FABMS: *m/z* 668 $[M]^+$; ^{1}H NMR ([D$_7$]DMF): δ = 8.18 (d, *J* = 8.6 Hz, 2H), 7.76 (d, *J* = 8.6 Hz, 2H), 7.59 (d, *J* = 7.6 Hz, 2H), 7.48 (m, 2H), 7.23 (m, 2H), 6.48 (d, *J* = 7.6 Hz, 2H), 4.25 (t, *J* = 4.5 Hz, 4H), 3.96 (t, *J* = 4.5 Hz, 4H), 3.75–3.50 (m, 20H), 3.17 (t, *J* = 6.4 Hz, 4H); ^{13}C NMR ([D$_7$]DMF): δ = 155.0, 135.2, 133.4, 127.9, 127.2, 126.9, 125.9, 123.7, 114.7, 106.4, 71.3, 71.2 (x2), 70.9, 70.0, 69.7, 68.8, 34.0; Anal. calcd for $C_{36}H_{44}O_8S_2$: C 64.7, H 6.63; found C 64.4, H 6.66.

1,30-Dithia-1,5-naphtho-*p*-phenylene[36]crown-10 (11): A mixture of 1,5-naphthalenedithiol (0.96 g, 5.0 mmol) and **9** (3.85 g, 5.0 mmol) in DMF (50 mL) was added at a constant rate during 24 h to a stirred suspension of Cs_2CO_3 (4.89 g, 15.0 mmol) in DMF (300 mL) at 70 °C under a nitrogen atmosphere, and the reaction mixture was stirred overnight at 70 °C. After workup and column chromatography (SiO_2, Et_2O/CH_2Cl_2/MeOH, 68:30:2) according to the procedure described for **2**, the macrocycle **11** was obtained as a white solid (682 mg, 22%) and crystallized from CH_2Cl_2/Et_2O (498 mg, 16%). m.p. 59 °C; FABMS: *m/z* 618 $[M]^+$; ^{1}H NMR ([D$_7$]DMF): δ = 8.24 (d, *J* = 8.5 Hz, 2H), 7.69 (d, *J* = 7.1 Hz, 2H), 7.56 (m, 2H), 6.76 (s, 4H), 3.99 (t, *J* = 4.6 Hz, 4H), 3.76 (t, *J* = 4.6 Hz, 4H), 3.72 (t, *J* = 6.4 Hz, 4H), 3.65–3.55 (m, 16H), 3.25 (t, *J* = 6.4 Hz, 4H); ^{13}C NMR ([D$_7$]DMF): δ = 153.7, 135.3, 133.4, 127.9, 127.0, 123.7, 116.0, 71.2, 71.1 (2 signals), 70.9, 70.1, 69.8, 68.7, 34.0; Anal. calcd for $C_{32}H_{42}O_8S_2$: C 62.1, H 6.84; found C 62.1, H 6.86.

13,18-Dithia-1,5-naphtho-*p*-phenylene[36]crown-10 (12): A mixture of 1,4-benzenedithiol (710 mg, 5.0 mmol) and **8** (4.10 g, 5.0 mmol) in DMF (50 mL) was added at a constant rate during 24 h to a stirred suspension of Cs_2CO_3 (4.89 g, 15 mmol) in DMF (300 mL) at 70 °C under nitrogen, and the reaction mixture was stirred overnight at 70 °C. After workup and column chromatography (SiO_2, $MeCO_2Et$/CH_2Cl_2, 1:10) according to the procedure described for **2**, the macrocycle **12** was obtained as a white solid (680 mg, 22%) and crystallized from MeOH (556 mg, 18%). m.p. 49 °C; FABMS: *m/z* 618 $[M]^+$; ^{1}H NMR ($CDCl_3$): δ = 7.87 (d, *J* = 8.5 Hz, 2H), 7.29 (m, 2H), 7.08 (s, 4H), 6.82 (d, *J* = 7.5 Hz, 2H), 4.30 (t, *J* = 4.7 Hz, 4H), 4.00 (t, *J* = 4.7 Hz, 4H), 3.79 (m, 4H), 3.68 (m, 4H), 3.63 (m, 4H), 3.58 (t, *J* = 6.9 Hz, 4H), 3.53 (m, 4H), 2.94 (t, *J* = 6.9 Hz, 4H); ^{13}C NMR ($CDCl_3$): δ = 154.3, 133.7, 129.7, 126.7, 125.0, 114.6, 105.7, 71.1, 70.8, 70.7, 70.4, 69.7, 69.6, 68.0, 33.2; Anal. calcd for $C_{32}H_{42}O_8S_2$: C 62.1, H 6.84; found C 62.0, H 6.82.

1,30-Dithiabis-*p*-phenylene[34]crown-10 (13): A mixture of 1,4-benzenedithiol (710 mg, 5.0 mmol) and **9** (3.85 g, 5.0 mmol) in DMF (50 mL) was added at a constant rate during 24 h to a stirred suspension of Cs_2CO_3 (4.89 g, 15.0 mmol) in DMF (300 mL) at 70 °C under a nitrogen atmosphere, and the reaction mixture was stirred overnight at 70 °C. After workup and column chromatography (SiO_2, $MeCO_2Et$/CH_2Cl_2, 1:10) according to the procedure described for **2**, the macrocycle **13** was obtained as an oil (653 mg, 23%) and crystallized from CH_2Cl_2/Et_2O (398 mg, 14%). m.p. 51 °C; EIMS: *m/z* 568 $[M]^+$; ^{1}H NMR ($CDCl_3$): δ = 7.22 (s, 4H), 6.82 (s, 4H), 4.07 (t, *J* = 4.8 Hz, 4H), 3.83 (t, *J* = 4.8 Hz, 4H), 3.74–3.56 (m, 20H), 3.05 (t, *J* = 6.9 Hz, 4H); ^{13}C NMR ($CDCl_3$): δ = 153.1, 134.0, 129.9, 115.7, 70.9, 70.8, 70.7, 70.5, 69.8, 69.7, 68.3, 33.4; Anal. calcd for $C_{28}H_{40}O_8S_2$: C 59.1, H 7.09; found C 59.0, H 6.95.

1,5-Bis(2-(2-methoxyethoxy)ethanethio)naphthalene (14): 1,5-Naphthalenedithiol (1.92 g, 10.0 mmol) and 1-chloro-2-(2-methoxyethoxy)ethane (2.77 g, 20.0 mmol) were added to a suspension of K_2CO_3 (4.14g, 30.0 mmol) in dry MeCN (250 mL) under a nitrogen atmosphere, and the whole was heated under reflux for 24 h. After cooling, the solvent was evaporated in vacuo, and the residue was treated with CH_2Cl_2 (250 mL) and washed with H_2O (3 × 200 mL). The organic phase was concentrated and subjected to column chromatography (SiO_2, $MeCO_2Et$/CH_2Cl_2, 1:19), giving the compound **14** as a pale yellow oil (2.93 g, 74%). EIMS: *m/z* 396 $[M]^+$; ^{1}H NMR ($CDCl_3$): δ = 8.38 (d, *J* = 8.5 Hz, 2H), 7.66 (d, *J* = 7.5 Hz, 2H), 7.46 (m, 2H), 3.65 (t, *J* = 7 Hz, 4H), 3.46–3.59 (m, 8H), 3.36 (s, 6H), 3.17 (t, *J* = 7 Hz, 4H); ^{13}C NMR ($CDCl_3$): δ = 133.9, 133.8, 129.3, 125.9, 124.8, 71.9, 70.3, 69.9, 59.0, 33.9; HRMS calcd for $[M]^+$ ($C_{20}H_{28}O_4S_2$) 396.1429, found 396.1436.

1,5-Bis(2-(2-methoxyethanethio)ethoxy)naphthalene (16): A mixture of 1,5-bis(2-bromoethoxy)naphthalene (1.31 g, 3.50 mmol), 2-mercaptoethanol (547 mg, 0.70 mmol), and K_2CO_3 (966 mg, 7.0 mmol) in MeCN (200 mL) was heated under reflux for 12 h under nitrogen. After cooling, the solvent was replaced by CH_2Cl_2 (200 mL) and the mixture was filtered over Celite. Evaporation of the filtrate gave 1,5-bis(2-(2-hydroxyethanethio)ethoxy)-naphthalene as a white solid, which was crystallized from Et_2O (1.06 g, 82%). m.p. 82 °C; EIMS: *m/z* 368 $[M]^+$; ^{1}H NMR ($CDCl_3$): δ = 7.84 (d, *J* = 8.5 Hz, 2H), 7.34 (m, 2H), 6.85 (d, *J* = 7.5 Hz, 2H), 4.33 (t, *J* = 6.5 Hz, 4H), 3.80 (t, *J* = 5.9 Hz, 4H), 3.07 (t, *J* = 6.5 Hz, 4H), 2.88 (t, *J* = 5.9 Hz, 4H), 2.15 (s, 2H); ^{13}C NMR ($CDCl_3$): δ = 154.0, 126.8, 125.2, 114.7, 105.9, 68.2, 60.7, 35.9, 30.9.

The resulting compound (736 mg, 2.0 mmol) was added to a suspension of NaH in dry THF (50 mL) under a nitrogen atmosphere, and the whole was stirred vigorously for 40 min at room temperature. Then, MeI (0.71 g, 5.0 mmol) was added and the reaction mixture was stirred for 16 h. The excess of NaH was quenched by the addition of H_2O (120 mL), and the resulting solution was concentrated to 80 mL and extracted with CH_2Cl_2 (3 × 100 mL). The combined extracts were washed with H_2O (200 mL) and dried ($MgSO_4$). The solvent was evaporated off and the residue was crystallized from MeOH to give compound **16** as a white powder (681 mg, 86%): m.p. 59 °C; EIMS: *m/z* 396 $[M]^+$; ^{1}H NMR ($CDCl_3$): δ = 7.86 (d, *J* = 8.5 Hz, 2H), 7.36 (m, 2H), 6.84 (d, *J* = 7.5 Hz, 2H), 4.34 (t, *J* = 6.8 Hz, 4H), 3.63 (t, *J* = 6.5 Hz, 4H), 3.38 (s, 6H), 3.10 (t, *J* = 6.8 Hz, 4H), 2.88 (t, *J* = 6.5 Hz, 4H); ^{13}C NMR ($CDCl_3$): δ = 154.1, 126.8, 125.1, 114.6, 105.7, 72.3, 68.3, 58.7, 32.2, 31.6; Anal. calcd for $C_{20}H_{28}O_4S_2$: C 60.6, H 7.12; found C 60.4, H 6.98.

1,5-Bis(2-(2-(2-(methanethio)ethoxy)ethoxy)naphthalene (17): A suspension of 1,5-bis(2-(2-tosyloxyethoxy)ethoxy)naphthalene (1.61 g, 2.50 mmol) and MeSNa (0.70 g, 10.0 mmol) in MeCN (100 mL) was heated under reflux for 16 h under nitrogen. After cooling, the solvent was replaced by CH_2Cl_2 (200 mL) and the resulting mixture was washed with aqueous KOH (1 M, 100 mL) and H_2O (3 × 100 mL). After removal of the solvent, the residue was subjected to column chromatography (SiO_2, $MeCO_2Et$/CH_2Cl_2, 1:20) to give compound **17** as a white solid (957 mg, 97%), which was crystallized from MeOH. m.p. 62 °C; EIMS: *m/z* 396 $[M]^+$; ^{1}H NMR ($CDCl_3$): δ = 7.87 (d, *J* = 8.5 Hz, 2H), 7.34 (m, 2H), 6.83 (d, *J* = 7.5 Hz, 2H), 4.30 (t, *J* = 4.8 Hz, 4H), 3.94 (t, *J* = 4.8 Hz, 4H), 3.80 (t, *J* = 6.9 Hz, 4H), 2.75 (t, *J* = 6.9 Hz, 4H), 2.18 (s, 6H); ^{13}C NMR ($CDCl_3$): δ = 154.3, 126.8, 125.1, 114.7, 105.8, 71.0, 69.5, 68.0, 33.6, 16.0; Anal. calcd for $C_{20}H_{28}O_4S_2$: C 60.6, H 7.12; found C 60.5, H 7.07.

{[2]-[1,13,18,30-Tetrathiabis-*para*-phenylene[34]crown-10][cyclobis(paraquat-*p*-xylylene)]catenane}[PF$_6$]$_4$ (20·4PF$_6$): A solution of **4** (60 mg, 0.10 mmol), 1,4-(bisbromomethyl)benzene (79 mg, 0.30 mmol), and **18**·2PF$_6$ (212 mg, 0.30 mmol) in DMF (5 mL) was subjected to ultrahigh pressure (12 kbar) at 20 °C for 5 d. The solvent was removed in vacuo, and the resulting red solid was washed with CH_2Cl_2 (2 × 25 mL) and Et_2O (2 × 25 mL), and purified by column chromatography (SiO_2, MeOH/2M NH_4Cl/$MeNO_2$, 7:2:1) to give **20**·4PF$_6$, as a red solid (25 mg, 15%) after counterion exchange (NH_4PF_6/H_2O). m.p. > 250 °C; FABMS: *m/z* 1723 $[M+Na]^+$, 1700 $[M]^+$, 1555 $[M-PF_6]^+$, 1410 $[M-2PF_6]^+$, 1265 $[M-3PF_6]^+$; ^{1}H NMR (CD_3CN, 25 °C): δ = 8.90 (d, *J* = 6.5 Hz, 8H), 7.81 (s+d, 16H), 5.72 (s, 8H), 6.43–4.44 (v br, 8H), 3.82 (br t, 8H), 3.74 (br t, 8H), 3.64 (t, *J* = 5.8 Hz, 8H), 2.72 (t, *J* = 5.8 Hz, 8H); Anal. calcd for $C_{64}H_{72}F_{24}N_4O_6S_4P_4$: C 45.2, H 4.27, N 3.29; found C 45.1, H 4.42, N 3.35.

General Procedures for the Synthesis of the [2]Catenanes 21·4PF$_6$–25·4PF$_6$: *Method A*: 1,4-Bis(bromomethyl)benzene (0.20 mmol) in DMF (5 mL) was added to a solution of **18**·2PF$_6$ (0.20 mmol) and the macrocyclic polythioether (2.6 molequiv) in DMF (15 mL), and the reaction mixture was stirred under a nitrogen atmosphere. After a few hours, a red/purple color appeared, followed by the precipitation of a red/purple solid. Stirring was continued for 4 d at room temperature. Then, the solvent was evaporated off under reduced pressure to give a colored residue, which was purified by column chromatography (SiO_2, MeOH/2M NH_4Cl/$MeNO_2$, 7:2:1). The fractions containing the [2]catenane (as monitored by TLC) were combined and evaporated in vacuo to give a residue, which was dissolved in H_2O (250 mL). The [2]catenane was precipitated from this solution by ion exchange with NH_4PF_6, and isolated as an intense colored solid.

0947-6539/97/0305-0784 $ 17.50+.50/0 Chem. Eur. J. 1997, 3, No. 5

Method B: A stirred solution of the macrocyclic polythioether (0.20 mmol) in DMF (20 mL) at room temperature under nitrogen was treated with three portions of **18**·2PF_6 (total 6 molequiv) and 1,4-bis(bromomethyl)benzene (total 6 molequiv) at intervals of 2 d. Stirring was continued for an additional 2 d. Evaporation of the solvent under reduced pressure gave an intense colored residue, which was washed with CH_2Cl_2 and Et_2O, and dissolved in H_2O (200 mL). The [2]catenane was precipitated from this solution by the addition of NH_4PF_6, and purified by column chromatography (SiO_2, MeOH/2 M NH_4Cl/$MeNO_2$, 7:2:1).

{[2]-[1,13,20,32-Tetrathiabis-1,5-naphtho[38]crown-10][cyclobis(paraquat-*p*-xylylene)]catenane}[PF_6]$_4$ (**21**·4PF_6): This catenane was prepared from **5** as a purple solid in 47% yield using method A and in 70% yield using method B. m.p. > 250 °C; FABMS: *m/z* 1800 $[M]^+$, 1655 $[M-PF_6]^+$, 1510 $[M-2PF_6]^+$, 1365 $[M-3PF_6]^+$; ^{1}H NMR (CD_3CN, 22 °C): δ = 8.91 (br, 4H), 8.37 (br, 4H), 7.96 (br, 8H), 7.37 (d, 2H), 7.14 (t, 2H), 7.0–6.70 (br, 8H), 6.77 (d, 2H), 6.50 (d, 2H), 5.94 (t, 2H), 5.90–5.60 (br, 8H), 4.12 (br, 4H), 4.05–3.70 (br, 20H), 3.30 (br, 4H), 2.93 (br, 4H), 2.23 (d, 2H); ^{1}H NMR (CD_3CN, −35 °C): δ = 8.86 (d, *J* = 6.5 Hz, 4H), 8.31 (br d, 4H), 8.05 (s, 4H), 7.80 (s, 4H), 7.24 (d, *J* = 8.3 Hz, 2H), 7.08 (m, 2H), 6.90 (br, 4H), 6.70 (br, 4H), 6.64 (d, *J* = 7.6 Hz, 2H), 6.40 (d, *J* = 7.6 Hz, 2H), 5.87 (m, 2H), 5.81 (d, *J* = 13.5 Hz, 4H), 5.63 (d, *J* = 13.5 Hz, 4H), 4.10 (br, 4H), 3.95–3.65 (br, 20H), 3.26 (br, 4H), 2.89 (br, 4H), 2.04 (d, *J* = 8.3 Hz, 2H); Anal. calcd for $C_{72}H_{76}F_{24}N_4O_6S_4P_4 \cdot 4H_2O$: C 46.2, H 4.52, N 2.99; found C 46.4, H 4.17, N 2.92.

{[2]-[1,32-Dithiabis-1,5-naphtho[38]crown-10][cyclobis(paraquat-4,4′-xylylene)]catenane}[PF_6]$_4$ (**22**·4PF_6): This catenane was prepared from **10** as a purple solid in 60% yield using method A and in 77% yield using method B. m.p. > 250 °C; FABMS: *m/z* 1768 $[M]^+$, 1623 $[M-PF_6]^+$, 1478 $[M-2PF_6]^+$, 1333 $[M-3PF_6]^+$; ^{1}H NMR (CD_3CN, 20 °C): δ = 8.94, 8.84, 8.40, 8.35 (br + d + d + br, *J* = 6.5 Hz, 8H), 8.14–7.82 (m, 8H), 7.13–6.61 (m, 8H), 5.90–5.63 (m, 8H), 7.41, 2.2 (2d, *J* = 8.2 Hz, 2H), 7.19, 2.27 (2d, *J* = 8.2 Hz, 2H), 7.18, 5.94 (2t, *J* = 8.2/7.6 Hz, 2H), 7.09, 5.83 (2t, *J* = 8.2/7.6 Hz, 2H), 6.87, 6.49 (2d, *J* = 7.6 Hz, 2H), 6.29, 6.12 (2d, *J* = 7.6 Hz, 2H), 4.25–3.65 (m, 28H), 3.30 (br t, 2H), 2.90 (br t, 2H); Anal. calcd for $C_{72}H_{76}F_{24}N_4O_8S_2P_4$: C 48.9, H 4.33, N 3.17; found C 48.5, H 4.25, N 3.46.

{[2]-[1,30-Dithia-1,5-naphtho-*para*-phenylene[36]crown-10][cyclobis(paraquat-*p*-xylylene)]catenane}[PF_6]$_4$ (**23**·4PF_6): This catenane was prepared from **11** as a purple solid in 50% yield using method A and in 65% yield using method B. m.p. > 250 °C; FABMS: *m/z* 1718 $[M]^+$, 1573 $[M-PF_6]^+$, 1428 $[M-2PF_6]^+$, 1283 $[M-3PF_6]^+$; ^{1}H NMR (CD_3CN, 21 °C): δ = 9.13–8.44 (m, 8H), 8.12–7.74 (m, 8H), 7.50–6.95 (m, 8H), 5.9–5.5 (m, 8H), 7.55, 2.31 (br d, 2H), 7.26, 6.05 (br t, 2H), 6.94, 6.56 (br d, 2H), 6.05, 3.36 (br s, 4H), 4.22–3.21 (m, 30H), 2.92 (br, 2H); ^{1}H NMR (CD_3CN, 0 °C): δ = 8.97, 8.73, 8.48 (3d, *J* = 6.5 Hz, 8H), 7.96, 7.76 (br + s, 8H), 7.42, 7.12, 7.0 (3d, *J* = 6.5 Hz, 8H), 5.77, 5.69, 5.68 (d + d + s, *J* = 13.5 Hz, 8H), 7.50, 2.25 (2d, *J* = 8.4 Hz, 2H), 7.24, 6.03 (2t, *J* = 8.4/7.6 Hz, 2H), 6.89, 6.54 (2d, *J* = 7.6 Hz, 2H), 6.0, 3.3 (s + br, 4H), 4.13 (br, 2H), 4.0–3.4 (m, 24H), 3.4–3.2 (m, 4H), 2.91 (br, 2H); Anal. calcd for $C_{68}H_{74}F_{24}N_4O_8S_2P_4$: C 47.5, H 4.34, N 3.26; found C 47.2, H 4.33, N 3.20.

{[2]-[13,18-Dithia-1,5-naphtho-*para*-phenylene[36]crown-10][cyclobis(paraquat-*p*-xylylene)]catenane}[PF_6]$_4$ (**24**·4PF_6): The catenane was prepared from **12** as a purple solid in 86% yield using method B. m.p. > 250 °C; FABMS: *m/z* 1718 $[M]^+$, $[M-PF_6]^+$, 1573 $[M-2PF_6]^+$, 1428 $[M-3PF_6]^+$; ^{1}H NMR (CD_3CN): δ = 8.95 (d, *J* = 6.5 Hz, 4H), 8.57 (d, *J* = 6.5 Hz, 4H), 8.10 (s, 4H), 7.94 (s, 4H), 7.16 (d, *J* = 6.5 Hz, 4H), 7.14 (d, *J* = 6.5 Hz, 4H), 6.53 (s, 4H), 6.21 (d, *J* = 7.8 Hz, 2H), 5.94 (m, 2H), 5.82 (d, *J* = 13.5 Hz, 4H), 5.68 (d, *J* = 13.5 Hz, 4H), 4.27 (br, 4H), 4.18 (br, 4H), 4.06 (br, 4H), 3.92 (br, 4H), 3.81 (br, 4H), 3.65 (br, 4H), 3.42 (t, *J* = 6 Hz, 4H), 2.57 (t, *J* = 6 Hz, 4H), 2.42 (d, *J* = 8.1, 2H); Anal. calcd for $C_{68}H_{74}F_{24}N_4O_8S_2P_4$: C 47.5, H 4.34, N 3.26; found C 47.1, H 4.35, N 3.63.

{[2]-[1,30-Dithiabis-*para*-phenylene[34]crown-10][cyclobis(paraquat-*p*-xylylene)]catenane}[PF_6]$_4$ (**25**·4PF_6): This catenane was prepared from **13** as a purple solid in 53% yield using method B. m.p. > 250 °C; FABMS: *m/z* 1668 $[M]^+$, 1523 $[M-PF_6]^+$, 1378 $[M-2PF_6]^+$, 1233 $[M-3PF_6]^+$; ^{1}H NMR (CD_3CN): δ = 8.89 (d, *J* = 6.5 Hz, 8H), 7.81 (s, 8H), 7.66 (d, *J* = 6.5 Hz, 8H), 6.63 (br s, 4H), 5.70 (s, 8H), 3.96 (br, 4H), 3.92–3.82 (m, 12H), 3.69 (br, 4H), 3.60 (br, 4H), 3.52 (br s, 4H), 3.45 (t, *J* = 6 Hz, 4H), 2.60 (t, *J* = 6 Hz, 4H); Anal. calcd for $C_{64}H_{72}F_{24}N_4O_8S_2P_4$: C 46.1, H 4.35, N 3.36; found C 45.8, H 4.28, N 3.28.

X-Ray Crystallography: Single crystals of the macrocyclic polythioethers **2** and **10**, suitable for X-ray crystallographic analyses, were obtained as described in the experimental procedures of the individual compounds. Single crystals of the the [2]pseudorotaxane **17**/**27**·4PF_6 and the [2]catenanes **20**·4PF_6, **21**·4PF_6, **23**·4PF_6, and **24**·4PF_6, suitable for X-ray crystallographic analyses, were grown by vapor diffusion of *i*Pr_2O in MeCN solutions of equimolar amounts of **17** and **27**·4PF_6—in the case of **17**/**27**·4PF_6—or the [2]catenanes—in the case of **20**·4PF_6, **21**·4PF_6, **23**·4PF_6, and **24**·4PF_6. The crystal data, data collection, and refinement parameters for the macrocycles **2** and **10**, the [2]pseudorotaxane **17**/**27**·4PF_6, and the [2]catenanes **20**·4PF_6–**24**·4PF_6 are summarized in Tables 9 and 10. All the structures were solved by direct methods and were refined by full-matrix least-squares based on F^2. For structures **2**, **17**/**27**·4PF_6, **20**·4PF_6, **21**·4PF_6, and **23**·4PF_6 all the major occupancy non-hydrogen atoms were refined anisotropically. As a result of limited data and severe disorder, respectively, in **24**·4PF_6 the solvent molecules and the carbon atoms of the tetracationic cyclophane component and in **10** (which has two 50% occupancy molecules disordered over two crystallographically independent centers of symmetry) the carbons atoms of the optimized naphthalene rings were refined isotropically. The remaining major occupancy non-hydrogen atoms in these two structures were refined anisotropically. The structures **17**/**27**·4PF_6 and **24**·4PF_6 have disordered polythioether chains (the major occupancy conformation is that illustrated) and **17**/**27**·4PF_6, **21**·4PF_6, **23**·4PF_6, and **24**·4PF_6 contain disordered hexafluorophosphate anions—each disorder was resolved into alternate partial occupancy orientations. All of the C–H hydrogen atoms in each of the seven structures were placed in calculated positions, assigned isotropic thermal parameters, $U(H) = 1.2\,U_{eq}(C)$, and allowed to ride on their parent atoms. Computations were carried out using the SHELXTL PC program system.[20] Crystallographic data (excluding structure factors) for the structures reported in this paper have been deposited with the Cambridge Crystallographic Data Centre as supplementary publication no. CCDC-100163. Copies of the data can be obtained free of charge on application to The Director, CCDC, 12 Union Road, Cambridge CB21EZ, UK (Fax: Int. code + (1223) 336-033; e-mail: deposit@chemcrys.cam.ac.uk).

General Method for the Determination of the Association Constants by UV/Vis Spectroscopy Employing the Titration Methodology: A series of MeCN solutions with constant concentration of the host (ca. 10^{-3} M) and containing different amounts of the guest (ca. 10^{-4}–10^{-2} M) were prepared. The absorbance at the wavelength (λ_{max}) corresponding to the maximum of the charge-transfer band for the 1:1 complex was measured for all the solutions. The correlation between absorbance and guest concentration was used to evaluate the association constant (K_a) by a nonlinear curve-fitting program.[21]

General Method for the Determination of the Association Constants by ^{1}H NMR Spectroscopy Employing the Continuous Variations Methodology: Two MeCN solutions, one containing **26**·2PF_6 and the other the macrocyclic polythioether were prepared with identical concentrations (ca. 10^{-3} M). From these two stock solutions, several new solutions with the same total volumes, but differing in the ratios of the two components (from 1:9 to 9:1, host:guest), were prepared. The chemical shifts of the aromatic protons of the macrocyclic polyethers were measured by ^{1}H NMR spectroscopy at 25 °C. The correlation between the mole fraction of the guest and the chemical shift change was used to evaluate the association constant (K_a) by a nonlinear curve-fitting program.[21]

Electrochemistry: The electrochemical measurements were obtained by using a Princeton Applied Research (PAR) Model 273A equipped with a saturated calomel electrode, as the reference electrode, a glassy carbon electrode, as the working electrode, and a platinum electrode, as the counter electrode. Cyclic voltammograms were recorded and analyzed at room temperature using the EG & G Model 250/270 electrochemical analysis software. Experiments were performed in deareated MeCN solutions under a nitrogen atmosphere. Analyte concentrations were held constant in the 0.1–0.5 mM range. Measurements were conducted in a standard single-compartment cell. Tetrabutylammonium hexafluorophosphate (0.1 M) was used as the supporting electrolyte.

Table 9. Crystal data, data collection, and refinement parameters [a].

	2	**10**	**17/26**·4PF$_6$
formula	$C_{28}H_{40}O_6S_4$	$C_{36}H_{44}O_8S_2$	$C_{76}H_{88}N_4O_8S_4$·4PF$_6$
solvent	–	–	6MeCN
formula weight	600.8	668.8	2140.0
color, habit	clear thin needles	straw tabular prismatic	deep red cubes
crystal size (mm)	0.70 × 0.27 × 0.05	0.60 × 0.33 × 0.06	0.50 × 0.40 × 0.32
lattice type	triclinic	triclinic	triclinic
space group	$P\bar{1}$	$P\bar{1}$	$P\bar{1}$
T (K)	293	293	293
a (Å)	8.322(1)	9.017(9)	13.535(2)
b (Å)	10.694(1)	12.102(12)	13.762(1)
c (Å)	17.418(2)	16.62(2)	14.458(2)
α (°)	90.85(1)	83.31(8)	88.28(1)
β (°)	96.45(1)	76.05(8)	80.01(1)
γ (°)	97.96(1)	74.69(8)	74.00(1)
V (Å^3)	1524.7(3)	1695(3)	2549.0(4)
Z	2	2 [b]	1 [c]
ρ_{calcd} (g cm^{-3})	1.309	1.311	1.394
F(000)	640	712	1108
radiation used	$Mo_{K\alpha}$	$Cu_{K\alpha}$	$Cu_{K\alpha}$
μ (mm^{-1})	0.350	1.845	2.334
θ range (°)	1.9–25.0	2.7–60.0	3.1–60.0
no. of unique reflections			
measured	5350	5009	7573
observed, $\|F_o\| > 4\sigma(\|F_o\|)$	3447	3290	5314
no. of variables	344	534	679
R_1 [d]	0.040	0.096	0.073
wR_2 [e]	0.093	0.260	0.195
weighting factors a, b [f]	0.047, 0.000	0.132, 1.753	0.104, 2.292
largest difference peak, hole (e Å^{-3})	0.20, −0.16	0.33, −0.28	0.38, −0.40

[a] Details in common: graphite monochromated radiation, ω scans, Siemens P4 diffractometer, refinement based on F^2. [b] There are two crystallographically independent C_i symmetric molecules in the asymmetric unit. [c] The molecule has crystallographic C_i symmetry. [d] $R_1 = \sum||F_o| - |F_c||/\sum|F_o|$. [e] $wR_2 = \sqrt{\{\sum[w(F_o^2 - F_c^2)^2]/\sum[w(F_o^2)^2]\}}$. [f] $w^{-1} = \sigma^2(F_o^2) + (aP)^2 + bP$.

Table 10. Crystal data, data collection, and refinement parameters for the [2]catenanes [a].

	20·4PF$_6$	**21**·4PF$_6$	**23**·4PF$_6$	**24**·4PF$_6$
formula	$C_{64}H_{72}N_4O_6S_4$·4PF$_6$	$C_{72}H_{76}N_4O_6S_4$·4PF$_6$	$C_{68}H_{74}N_4O_8S_2$·4PF$_6$	$C_{68}H_{74}N_4O_8S_2$·4PF$_6$
solvent	4MeCN	3.5MeCN·1.5PhH	8.5MeCN	4MeCN
formula weight	1865.6	2062.3	2068.3	1883.5
color, habit	purple blocks	red prisms	red platy needles	purple platy needles
crystal size (mm)	0.50 × 0.33 × 0.20	0.50 × 0.33 × 0.13	0.48 × 0.32 × 0.11	0.83 × 0.33 × 0.08
lattice type	monoclinic	triclinic	monoclinic	monoclinic
space group	$C2/c$	$P\bar{1}$	$P2_1/n$	$C2/c$
T (K)	293	293	183	293
a (Å)	23.624(2)	10.811(1)	17.633(3)	23.131(2)
b (Å)	13.846(2)	13.677(1)	31.287(2)	13.823(2)
c (Å)	27.546(3)	32.823(1)	18.052(2)	27.881(4)
α (°)	–	101.12(1)	–	–
β (°)	108.32(1)	95.60(1)	99.24(1)	108.00(1)
γ (°)	–	92.06(1)	–	–
V (Å^3)	8553(2)	4731.6(3)	9830(2)	8478(2)
Z	4 [b]	2	4	4 [b]
ρ_{calcd} (g cm^{-3})	1.449	1.448	1.398	1.476
F(000)	3840	2128	4276	3880
radiation used	$Cu_{K\alpha}$	$Cu_{K\alpha}$ [c]	$Cu_{K\alpha}$ [c]	$Cu_{K\alpha}$
μ (mm^{-1})	2.670	2.471	2.023	2.270
θ range (°)	3.4–57.0	1.4–55.0	2.9–55.0	3.3–63.0
no. of unique reflections				
measured	5540	11728	11925	5918
observed, $\|F_o\| > 4\sigma(\|F_o\|)$	3058	7930	6295	2551
no. of variables	534	1322	1279	479
R_1 [d]	0.093	0.084	0.110	0.114
wR_2 [e]	0.246	0.224	0.271	0.286
weighting factors a, b [f]	0.131, 25.420	0.130, 12.024	0.169, 34.821	0.166, 58.615
largest difference peak, hole (e Å^{-3})	0.45, −0.29	1.05, −0.57	0.78, −0.46	0.43, −0.46

[a] Details in common: graphite monochromated radiation, ω scans, Siemens P4 diffractometer, refinement based on F_o^2. [b] The molecule has crystallographic C_2 symmetry. [c] Rotating anode source. [d] $R_1 = \sum||F_o| - |F_c||/\sum|F_o|$. [e] $wR_2 = \sqrt{\{\sum[w(F_o^2 - F_c^2)^2]/\sum[w(F_o^2)^2]\}}$. [f] $w^{-1} = \sigma^2(F_o^2) + (aP)^2 + bP$.

A glassy carbon electrode (28 mm^2, EG & G) was used as the working electrode; its surface was routinely polished with a 0.5 μ alumina slurry on a felt surface immediately prior to use. All potentials were recorded against an EG & G PARC standard calomel electrode, and a platinum coil was used as the counter electrode. The cell potential was cycled from 0 to −1.2V (vs. SCE) for all samples.

Acknowledgments: Financial support from the Engineering and Physical Sciences Research Council, the NFWO, the University of Leuven, and the Ministerie voor wetenschapsbeleid is gratefully acknowledged. This research has been accomplished with fellowships from the IWT (for J. N.) and the University of Leuven (for W. D.).

Received: November 20, 1996 [F 524]

[1] a) D. Philp, J. F. Stoddart, *Synlett* **1991**, 445–458; b) D. Pasini, F. M. Raymo, J. F. Stoddart, *Gazz. Chim. Ital.* **1995**, *125*, 431–443; c) D. B. Amabilino, F. M. Raymo, J. F. Stoddart, *Comprehensive Supramolecular Chemistry*, Vol. 9 (Eds.: M. W. Hosseini, J.-P. Sauvage), Pergamon, Oxford, **1996**, pp. 85–130.

[2] a) P. R. Ashton, M. A. Blower, S. Iqbal, C. H. McLean, J. F. Stoddart, M. S. Tolley, D. J. Williams, *Synlett* **1994**, 1059–1062; b) P. R. Ashton, M. A. Blower, C. H. McLean, J. F. Stoddart, M. S. Tolley, *ibid.* **1994**, 1063–1066; c) P. R. Ashton, J. A. Preece, J. F. Stoddart, M. S. Tolley, A. J. P. White, D. J. Williams, *Synthesis* **1994**, 1344–1352; d) D. B. Amabilino, P. R. Ashton, C. L. Brown, E. Córdova, L. A. Godínez, T. T. Goodnow, A. E. Kaifer, S. P. Newton, M. Pietraszkiewicz, D. Philp, F. M. Raymo, A. S. Reder, M. T. Rutland, A. M. Z. Slawin, N. Spencer, J. F. Stoddart, D. J. Williams, *J. Am. Chem. Soc.* **1995**, *117*, 1271–1293; e) D. B. Amabilino, P. L. Anelli, P. R. Ashton, G. R. Brown, E. Córdova, L. A. Godínez, W. Hayes, A. E. Kaifer, D. Philp, A. M. Z. Slawin, N. Spencer, J. F. Stoddart, M. S. Tollley, D. J. Williams, *ibid.* **1995**, *117*, 11142–11170; f) P. R. Ashton, R. Ballardini, V. Balzani, A. Credi, M. T. Gandolfi, S. Menzer, L. Pérez-García, L. Prodi, J. F. Stoddart, M. Venturi, A. J. P. White, D. J. Williams, *ibid.* **1995**, *117*, 11171–11197; g) P. R. Ashton, J. Huff, S. Menzer, I. W. Parsons, J. A. Preece, J. F. Stoddart, M. S. Tolley, A. J. P. White, D. J. Williams, *Chem. Eur. J.* **1996**, *2*, 31–44; h) M. Asakawa, P. R. Ashton, S. Menzer, F. M. Raymo, J. F. Stoddart, A. J. P. White, J. F. Stoddart, *ibid.* **1996**, *2*, 877–893.

[3] a) C. O. Dietrich-Buchecker, J.-P. Sauvage, *Chem. Rev.* **1987**, *87*, 795–810; b) C. O. Dietrich-Buchecker, J.-P. Sauvage, *Bioorg. Chem. Front.* **1991**, *2*, 195–248; c) J.-C. Chambron, C. O. Dietrich-Buchecker, J.-P. Sauvage, *Top. Curr. Chem.* **1993**, *165*, 131–162; d) D. H. Busch, N. A. Stephenson, *Coord. Chem. Rev.* **1990**, *100*, 119–156; e) D. H. Busch, *J. Inclusion Phenom.* **1992**, *12*, 389–395; f) C. A. Hunter, D. H. Purvis, *Angew. Chem. Int. Ed. Engl.* **1992**, *31*, 792–795; g) C. A. Hunter, *J. Am. Chem. Soc.* **1992**, *114*, 5303–5311; h) F. J. Carver, C. A. Hunter, R. J. Shannon, *J. Chem. Soc. Chem. Commun.* **1994**, 1277–1280; i) H. Adams, F. J. Carver, C. A. Hunter, *ibid.* **1995**, 809–810; j) S. Anderson, H. L. Anderson, J. K. M. Sanders, *Acc. Chem. Res.* **1993**, *26*, 389–395; k) G. Brodesser, R. Güther, R. Hoss, S. Meier, S. Ottens-Hildebrandt, J. Schmitz, F. Vögtle, *Pure Appl. Chem.* **1993**, *65*, 2325–2328; l) R. Hoss, F. Vögtle, *Angew. Chem. Int. Ed. Engl.* **1994**, *33*, 375–384; m) F. Vögtle, R. Jäger, M. Händel, S. Ottens-Hildebrandt, *Pure Appl. Chem.* **1996**, *68*, 225–232; n) A. G. Johnston, D. A. Leigh, R. J. Pritchard, M. D. Deegan, *Angew. Chem. Int. Ed. Engl.* **1995**, *34*, 1209–1212; o) A. G. Johnston, D. A. Leigh, L. Nezhat, J. P. Smart, M. D. Deegan, *ibid.* **1995**, *34*, 1212–1216; p) D. A. Leigh, K. Moody, J. P. Smart, K. J. Watson, A. M. Z. Slawin, *ibid.* **1996**, *35*, 306–310; q) M. Bělohradský, F. M. Raymo, J. F. Stoddart, *Collect. Czech. Chem. Commun.* **1996**, *61*, 1–43; r) F. M. Raymo, J. F. Stoddart, *Pure Appl. Chem.* **1996**, *68*, 313–322; s) M. Bělohradský, F. M. Raymo, J. F. Stoddart, *Collect. Czech. Chem. Commun.* **1997**, *62*, in press.

[4] a) P. L. Anelli, P. R. Ashton, R. Ballardini, V. Balzani, M. Delgado, M. T. Gandolfi, T. T. Goodnow, A. E. Kaifer, D. Philp, M. Pietraszkiewicz, L. Prodi, M. V. Reddington, A. M. Z. Slawin, N. Spencer, J. F. Stoddart, C. Vicent, D. J. Williams, *J. Am. Chem. Soc.* **1992**, *114*, 193–218.

[5] a) S. R. Cooper, *Acc. Chem. Res.* **1988**, *21*, 141–146; b) S. R. Cooper, *Structur. Bonding*, **1990**, *72*, 1–72; c) A. J. Blake, M. Schröder, *Adv. Inorg. Chem.* **1990**, *35*, 1–80.

[6] The [2]catenane **1**·4PF_6 was synthesized in yields of 70 and 78% when the first (see ref. [4]) and second synthetic procedures were employed, respectively.

[7] P. R. Ashton, E. J. T. Chrystal, J. P. Mathias, K. P. Parry, A. M. Z. Slawin, N. Spencer, J. F. Stoddart, D. J. Williams, *Tetrahedron Lett.* **1987**, *28*, 6367–6370.

[8] P. R. Ashton, C. L. Brown, E. J. T. Chrystal, T. T. Goodnow, A. E. Kaifer, K. P. Parry, D. Philp, A. M. Z. Slawin, N. Spencer, J. F. Stoddart, D. J. Williams, *J. Chem. Soc. Chem. Commun.* **1991**, 634–639.

[9] M. V. Reddington, A. M. Z. Slawin, N. Spencer, J. F. Stoddart, C. Vicent, D. J. Williams, *J. Chem. Soc. Chem. Commun.* **1991**, 630–634.

[10] **14**/**26**·4PF_6: cell dimensions $a = 11.155(1)$, $b = 20.126(1)$, and $c = 14.076(2)$ Å, space group $P2_1/n$. **16**/**26**·4PF_6: cell dimensions $a = 10.895(2)$, $b = 19.975(4)$, and $c = 13.966(2)$ Å, space group $P2_1/n$.

[11] K. N. Connors, *Binding Constants*, Wiley, New York, **1987**.

[12] a) B. L. Allwood, N. Spencer, H. Shahriari-Zavareh, J. F. Stoddart, D. J. Williams, *J. Chem. Soc. Chem. Commun.* **1987**, 1064–1066; b) M. Asakawa, P. R. Ashton, S. E. Boyd, C. L. Brown, R. E. Gillard, O. Kocian, F. M. Raymo, J. F. Stoddart, M. S. Tolley, D. J. Williams, *J. Org. Chem.* **1997**, *62*, 26–37.

[13] M. Asakawa, W. Dehaen, G. L'abbé, S. Menzer, J. Nouwen, F. M. Raymo, J. F. Stoddart, D. J. Williams, *J. Org. Chem.* **1996**, *61*, 9591–9595.

[14] J. Sandström, *Dynamic NMR Spectroscopy*, Academic Press, London, **1982**.

[15] In the case of the [2]catenane **23**·4PF_6, as a result of the complexity of its ^{1}H NMR spectra recorded over a wide range of temperatures (−40 to +80 °C), only a qualitative analysis of its dynamic properties was possible.

[16] P. R. Ashton, M. Blower, D. Philp, N. Spencer, J. F. Stoddart, M. S. Tolley, R. Ballardini, M. Ciano, V. Balzani, M. T. Gandolfi, L. Prodi, C. H. McLean, *New J. Chem.* **1993**, *17*, 689–695

[17] B. S. Furniss, A. J. Hannaford, P. W. G. Smith, A. R. Tatchell, *Practical Organic Chemistry*, Longman, New York, **1989**.

[18] R. Machinek, W. Lüttke, *Synthesis*, **1975**, 255–256.

[19] a) C. S. Marvel, P. D. Caesar, *J. Am. Chem. Soc.* **1951**, *73*, 1097–1099; b) S. Oae, H. Togo, *Bull. Chem. Soc. Jpn.* **1983**, *56*, 3802–3812.

[20] SHELXTL PC version 5.03, Siemens Analytical X-Ray Instruments, Inc., Madison, WI, 1994.

[21] UltraFit version 2.11.